Abdominal Imaging

Published online: 10 February 2015

Abdom Imaging (2015) 40:2486–2511
DOI: 10.1007/s00261-015-0363-6

PET/CT and MRI in the imaging assessment of cervical cancer

Joanna Kusmirek,[1] Jessica Robbins,[1] Hailey Allen,[1] Lisa Barroilhet,[2] Bethany Anderson,[3] Elizabeth A. Sadowski[1,2]

[1]Department of Radiology, University of Wisconsin, 600 Highland Avenue, Madison, WI 53792-3252, USA
[2]Obstetrics and Gynecology, University of Wisconsin, Madison, WI 53792-3252, USA
[3]Radiation Oncology, University of Wisconsin, Madison, WI 53792-3252, USA

Abstract

Imaging plays a central role in the evaluation of patients with cervical cancer and helps guide treatment decisions. The purpose of this pictorial review is to describe magnetic resonance (MR) imaging and positron emission tomography (PET)/computed tomography (CT) assessment of cervical cancer, including indications for imaging, important findings that may result in management change, as well as limitations of both modalities. The International Federation of Gynecology and Obstetrics cervical cancer staging system does not officially include imaging; however, the organization endorses the use of MR imaging and PET/CT in the management of patients with cervical cancer where these modalities are available. MR imaging provides the best visualization of the primary tumor and extent of soft tissue disease. PET/CT is recommended for assessment of nodal involvement, as well as distant metastases. Both MR imaging and PET/CT are used to follow patients post-treatment to assess for recurrence. This review focuses on the current MR imaging and PET/CT protocols, the utility of these modalities in assessing primary tumors and recurrences, with emphasis on imaging findings which change management and on imaging pitfalls to avoid. It is important to be familiar with the MR imaging and PET/CT appearance of the primary tumor and metastasis, as well as the imaging pitfalls, so that an accurate assessment of disease burden is made prior to treatment.

Key words: Cervical cancer—MRI—PET/CT—Radiotherapy

Correspondence to: Elizabeth A. Sadowski; *email:* esadowski@uwhealth.org

Cervical cancer affects women in their 30s and 40s predominately and is one of the most common causes of cancer death in women 35 years and younger [1–5]. Worldwide, over 500,000 cases of cervical cancer are diagnosed each year and seventy percent of cases occur in underdeveloped countries. There is a marked discrepancy in disease survival between developed and underdeveloped countries [3]. In sub-Sahara Africa, 65% of women with cervical cancer die of their disease, whereas 38% of women die due to cervical cancer in developed regions [1, 6]. The regional differences in survival are in part due to access to surgeons, radiation oncologists, and contemporary imaging modalities to diagnose, stage, and guide treatment of women with cervical cancer.

Magnetic resonance (MR) imaging and positron emission tomography (PET)/computed tomography (CT) are advanced imaging techniques which are used routinely in the staging and treatment monitoring of cervical cancer [7–15]. The goals of this pictorial review are to discuss the appropriate use of PET/CT and MR imaging in the diagnosis and treatment of cervical cancer, the imaging findings which guide treatment, and important pitfalls to avoid on PET/CT and MR imaging. Crafting a radiology report, which includes the imaging features which are important to the decision-making process, will assure the treatment plan is tailored to maximize the clinical outcome in women with cervical cancer.

Treatment of cervical cancer

Accurate determination of the extent of disease at the time of diagnosis is critical in establishing the appropriate treatment for a patient with cervical cancer (Fig. 1). Palliative care is recommended for women with distant metastatic spread. Treatment options for non-metastatic cervical cancer generally include surgical resection for

early stage disease (Stage IIA or less) and radiation therapy typically delivered with concurrent chemotherapy for locally advanced (Stage IIB or greater) or otherwise high-risk disease (imaging positive lymph nodes). At some centers, chemoradiotherapy rather than surgery is used as the primary treatment modality for women with early stage disease (IB2 and IIA) when there is a large tumor (> 4 cm). A general principle of therapy is to avoid utilizing both surgery and chemoradiation therapy for a particular patient, to limit the morbidity of treatment [16]. Advanced imaging techniques are therefore extremely valuable in triaging patients to surgery versus primary chemoradiation therapy based on such features as large tumor size (> 4 cm), clinically occult parametrial invasion, and lymph node involvement [17, 18]. Identification of pelvic and peri-aortic lymphadenopathy prior to initiating primary chemoradiotherapy is also critical, to ensure that the radiation treatment volume encompasses clinically involved and high-risk areas.

MR imaging in the assessment of cervical cancer: staging and treatment decision

The current International Federation of Gynecology and Obstetrics (FIGO) 2009 staging system remains a clinical staging system based on clinical gynecological examination, with the addition of an exam under anesthesia, cystoscopy, and endoscopy as clinically indicated [4, 19–21]. This system remains in place because cervical carcinoma is most prevalent in developing countries, where imaging resources are limited. However, clinical staging is most accurate in early stage disease, with approximately 85% accuracy in Stage IA to IB1. Beyond these early stages, clinical staging diminishes in accuracy to less than

Fig. 3. Example MR images from a patient with cervical cancer. **A** Sagittal T2-weighted image through the uterus and cervix depicting the large (>4 cm) cervical tumor (*white arrow*). Note the vagina is filled with some gel (*black arrows*). **B** Axial T2-weighted image at the level of the cervical tumor (*white arrow*). No obvious parametrial invasion is seen, with a dark rim of cervical stromal tissue (*black arrows*) containing the tumor. **C** Sagittal T1-weighted image post-contrast injection demonstrating mild enhancement of the larger cervical tumor (*white arrows*). **D** Axial T1-weighted image post-contrast injection demonstrating mild enhancement of the larger cervical tumor (white arrows) with a thin rim of cervical tissue (*black arrows*) containing the tumor. **E** DWI images of the cervical tumor (*white arrows*). The tumor is isointense on the B = 0 image, becoming hyperintense on the B = 500 and is dark on the ADC map signifying restricted diffusion. *B* bladder, *U* uterus, *FF* free fluid, *P* parametrial tissue. ▶

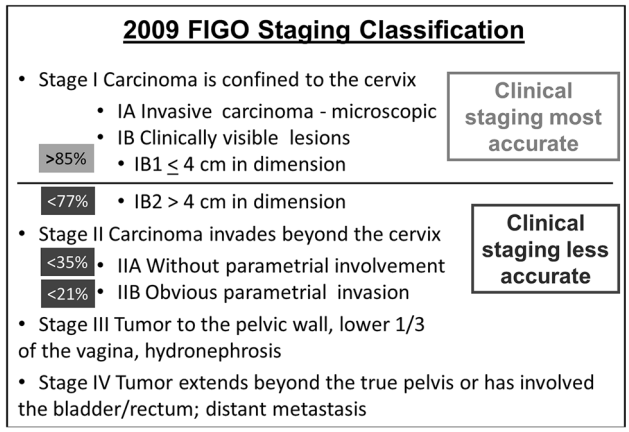

Fig. 2. Accuracy of FIGO clinical staging compared to surgical pathology.

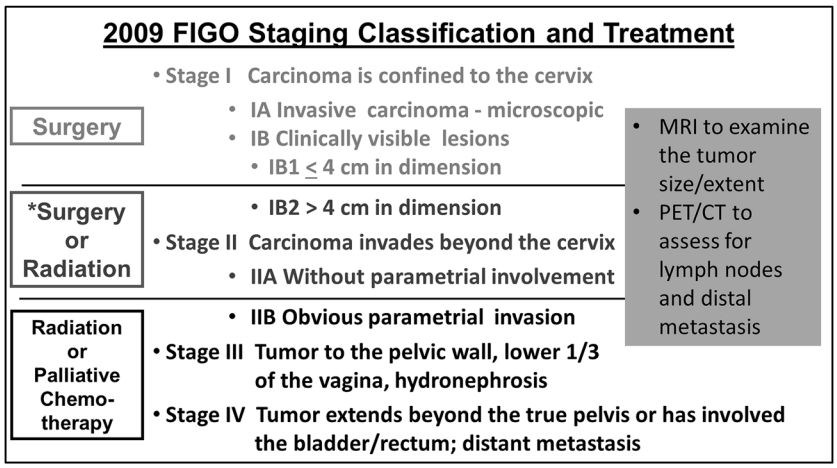

Fig. 1. First-line treatment based on MRI tumor evaluation and PET/CT assessment of lymph nodes and distal metastasis. * Some center will use chemoradiotherapy in stage IIB or greater, however, some centers will use chemoradiotherapy rather than surgery as the primary treatment modality for women with earlier stage disease (IB2 and IIA) when there is a larger tumor (>4 cm).

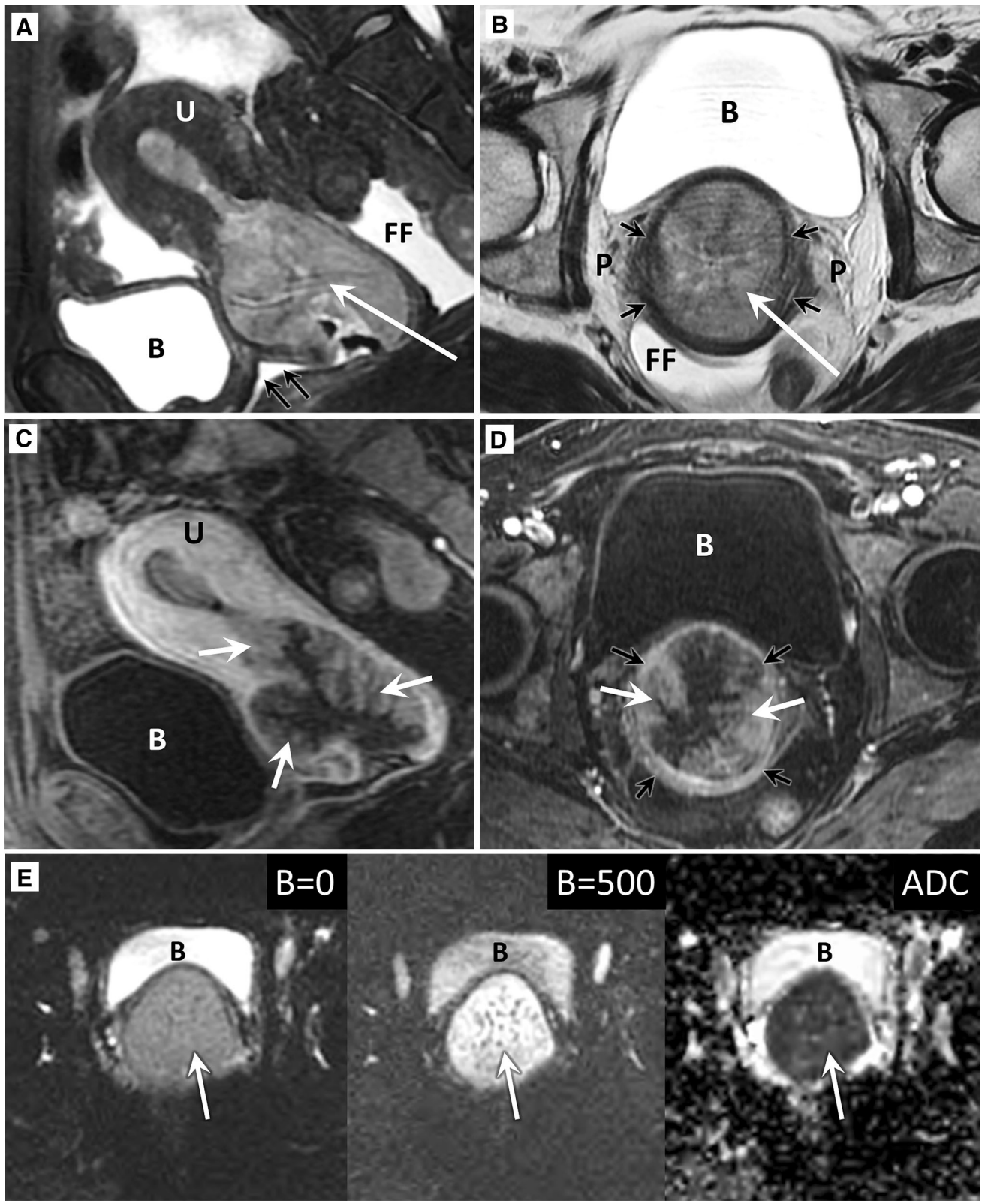
A
U
FF
B
B
B
P
P
FF
C
U
B
D
B
E
B=0
B
B=500
B
ADC
B

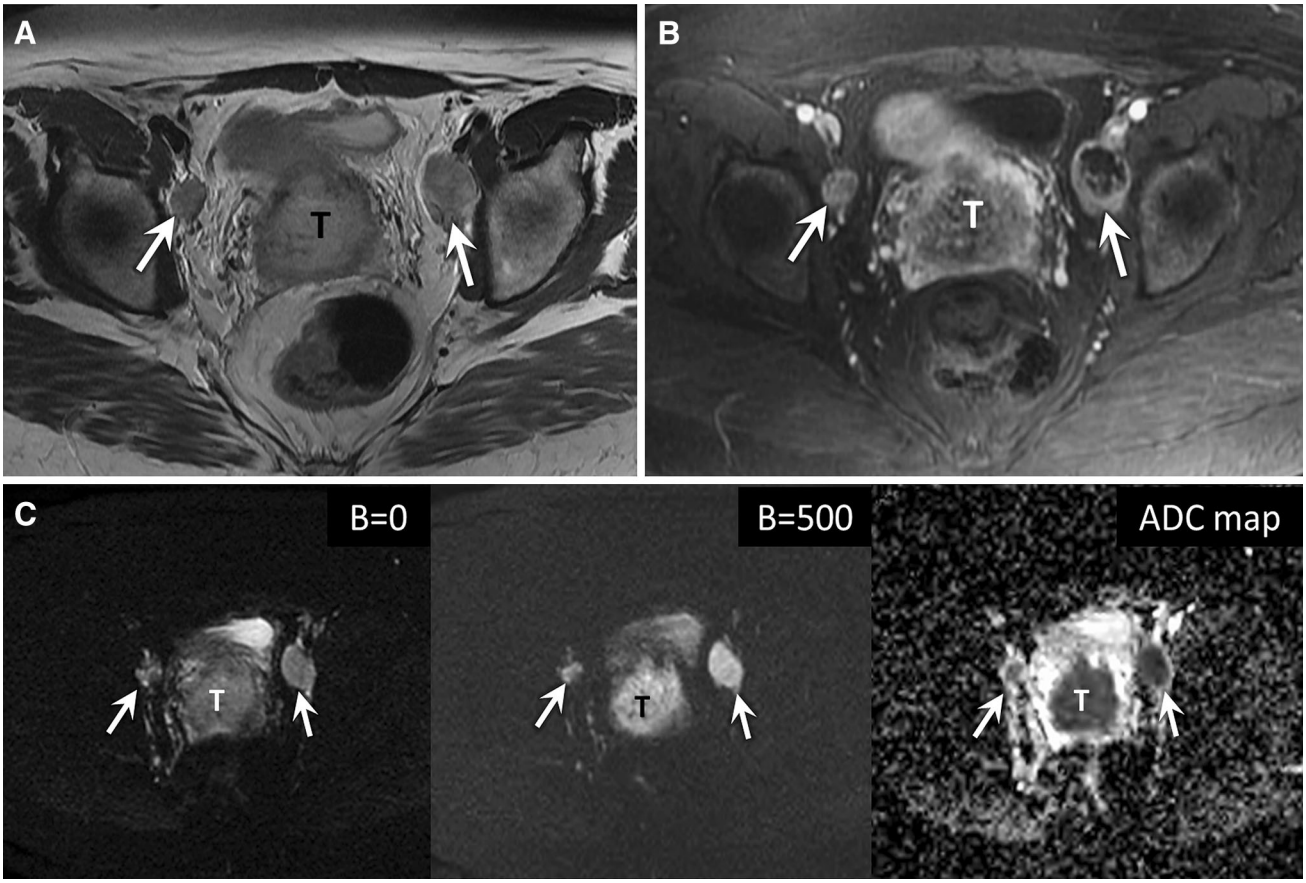

Fig. 4. 47-year-old female with clinical stage IIB cervical cancer, adenocarcinoma sub-type. **A** On MRI, axial T2-weighted image reveals enlarged isointense bilateral external iliac lymph nodes (*white arrows*). **B** Axial T1-weighted post-contrast image demonstrates enlarged enhancing, centrally necrotic external iliac lymph nodes (*white arrows*). **C** The diffusion-weighted images depict bilateral external iliac lymph nodes, which appear more hyperintense on the B = 500 image and dark on the ADC map (*white arrows*), signifying restricted diffusion. The primary tumor (*T*) is seen in the cervix.

35% in Stage IIA and 21% in Stage IIB (Fig. 2) [22]. Conversely, MR imaging has accuracy rates approaching 95% for stage IB or greater and is considered the single best modality by which to assess tumor size, location, and extension into the surrounding tissues [21, 23–28]. Due to the inaccuracies of clinical staging alone, FIGO recognizes the added utility of MR imaging. FIGO encourages the use of MR imaging, where available, in staging women with cervical cancer prior to definitive treatment and accepts MR imaging as a replacement of more invasive techniques such as cystoscopy and endoscopy for the evaluation of tumor extent to the bladder and rectum [8, 9, 11, 21, 22, 24–30].

When cervical cancer is first diagnosed, the role of MR imaging is to access tumor size, location, extent of invasion into adjacent structures and metastatic foci, including enlarged lymph nodes in the pelvis. MR imaging is used initially to decide the definitive first-line treatment (Fig. 1). Surgical resection is considered if the cervical tumor is confined to the cervix/upper vagina [4, 13, 25, 30–33]. Once the tumor extends beyond the cervix and upper vagina to involve the parametrium or lower vagina, it is considered a locally advanced disease (≥IIB), and chemotherapy-sensitized radiation therapy is the first-line treatment. At some centers, stage IB2 and stage IIA are also treated with chemoradiation therapy [5, 21,

Table 1. Example MR imaging protocol parameters for imaging patients with cervical cancer

Sequence	Axial T1	Sag T2	Axial T2	Axial T2	Axial DWI	Sag T2	Axial T1	Axial T1	Axial T1
Fat saturated (fat sat)		fat sat		fat sat		fat sat	fat sat	fat sat	fat sat
Time after injection of contrast (s)							40 s	90 s	180 s
Sequence	Fast Spin Echo	Fast Recovery Fast Spin Echo	Fast Recovery Fast Spin Echo	Fast Recovery Fast Spin Echo	Echoplanar	Fast Recovery Fast Spin Echo	Spoiled gradient echo	Spoiled gradient echo	Fast Spin Echo
Number of dimensions	2d	2d	2d	2d	2d	2d	3d	3d	2d
TE (ms)	9	90	86	90	65	90	1.8	1.8	9
TR (ms)	600	3400	3400	3800	10,000	3800	3.8	3.8	600
Echo train length	4	21	21	21		21	InvPrep TI = 20	InvPrep TI = 20	ETL 4
Flip angle (°)	90	90	90	90	90	90	12	12	90
Number of excitations (nex)	4	3	3	2	8	2	1	1	2
Bandwidth	27	31.25	31.25	31.25		31.25	62	62	27
FOV (cm)	26	26	26	34	32	32	28	28	32
Slice thickness/interval (mm)	5/1.5	5/1.5	5/1.5	6/1	3/0.5	5/1.5	4.6	4.6	6/1
Matrix size	256 × 224	320 × 256	320 × 256	320 × 256	160 × 160	256 × 224	256 × 192	256 × 192	256 × 192
b-Value (s/mm^2)					0, 500				
Approximate acquisition time	3:36	3:30	3:30	4:11	2:50	4:10	0:27	0:27	4:32
Location/coverage	Entire Pelvis	Entire Pelvis	Entire Pelvis	Below symphysis to mid kidneys	Pubic bone to crest	Entire uterus/ cervix	Entire pelvis	Entire pelvis	Below symphysis to mid kidneys

22, 28, 34]. MR imaging is also able to assess for lymph node metastasis with sensitivities up to 73% and specificities up to 96% [7, 25, 31, 33, 35–38]. Following initial definitive treatment, MR imaging may be used to guide brachytherapy, assess response to radiation treatment regimens, and to assess for recurrence following surgical resection or completion of the radiation treatments [5, 24, 39–43]. In the research arena, multi-parametric MR imaging is being used as a predictor of treatment response and prognosis, including disease-free survival and overall survival [5, 42, 44–50].

MR imaging protocol

Preparing patients for MR imaging studies includes fasting for 4–6 h prior to the examination. Small amounts of water with medications are allowed. At our institution, we do not administer an anti-peristaltic agent; however, some institutions do administer these agents prior to the exam to minimize bowel motion artifact. Immediately prior to imaging, gel is inserted into the vagina to improve visualization of the cervix. The patients are also instructed to void in order to minimize possible bladder-related artifacts. A comprehensive cervical cancer protocol should include the following sequences: pre-contrast axial T1-weighted images, axial and sagittal T2-weighted images, dynamic contrast-enhanced axial and sagittal T1-weighted images, and diffusion-weighted (DW) images; an example protocol is detailed in Table 1. Torso or cardiac coils are used for imaging the pelvis at many institutions, although dedicated pelvic coils can be used as well. Imaging can be performed on both 1.5 Tesla and 3 Tesla magnets.

MR imaging image analysis

Image analysis is performed on a dedicated digital image reading work station. The T2-weighted and DW images are the workhorse for evaluating the location, size, and extent of the primary tumor (Fig. 3). DW imaging is particularly useful when the tumor is small and difficult to visualize on the T2-weighted images or in a young patient where the cervical stroma is isointense and similar to cervical tumor signal [34, 50]. Post-contrast images do not improve the overall accuracy of staging compared to T2-weighted images alone; however, they are helpful in larger tumors, particularly when bladder, rectal, adnexal, or pelvic side wall invasion is suspected [21, 34, 49, 51].

Lymph nodes assessment on MR imaging is performed utilizing fat-saturated T2-weighted, DW, and T1-weighted post-contrast images. On the T2-weighted images, abnormal lymph nodes may be enlarged and can be seen as homogeneously hyperintense against the dark fat-saturated background or may be heterogeneous in

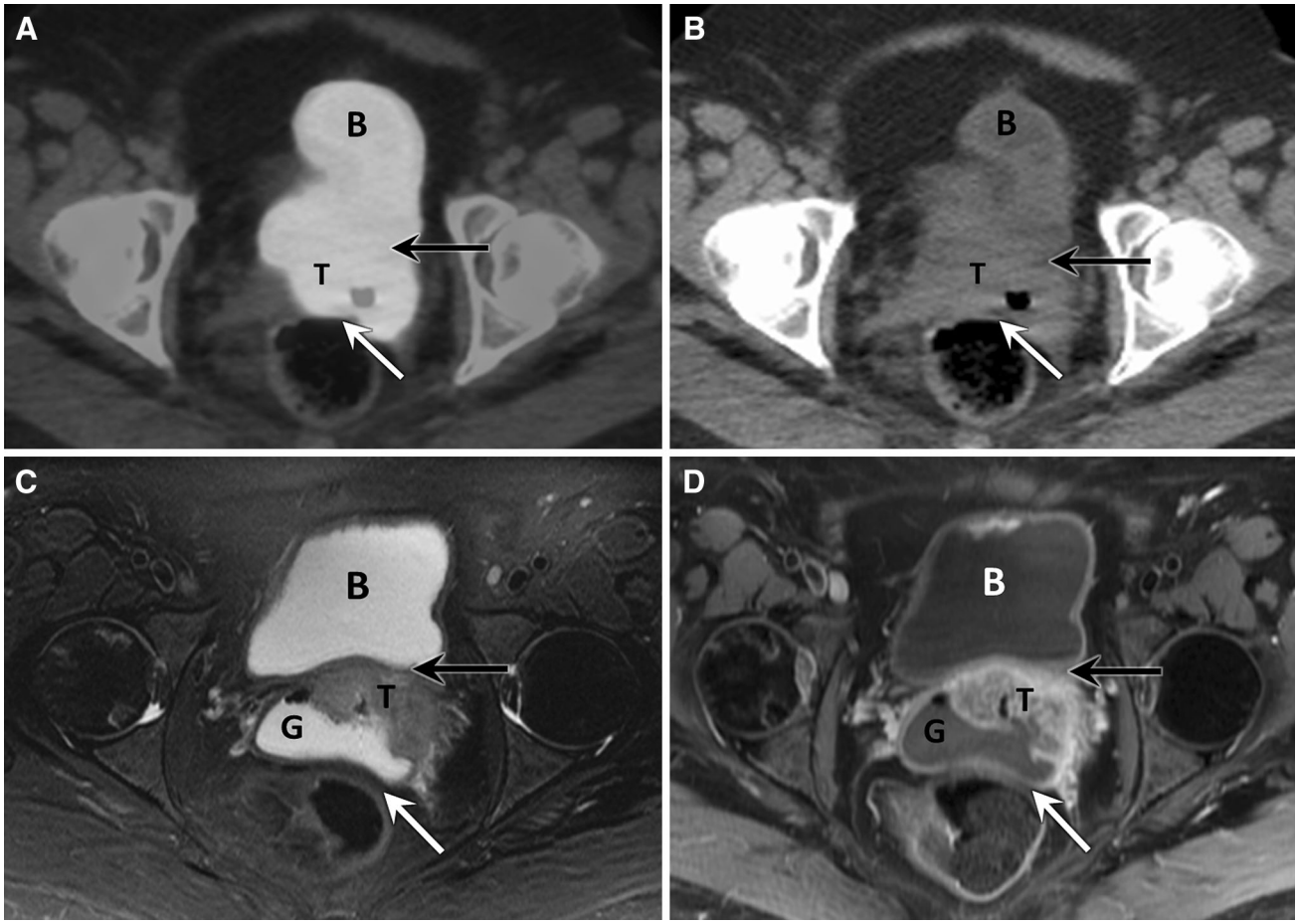

Fig. 5. 55-year-old female with stage IIB squamous cell cervical cancer. **A** Axial fused PET/CT image reveals a hypermetabolic cervical mass with poorly defined borders and no fat planes between the mass and the bladder anteriorly (*black arrow*) and the rectum posteriorly (*white arrow*). **B** Corresponding axial CT image without contrast depicts a cervical mass which is difficult to separate from the bladder wall (*black arrow*) and rectal wall (*white arrow*). **C** Axial T2-weighted image depicts the cervical tumor abutting the posterior wall of the bladder (*black arrow*), without definite invasion of the bladder. Gel distends the vagina, and the cervical tumor is seen to involve the anterior wall of the vagina only, away from the rectum (*white arrow*). **D** Axial T1-weighted image post-contrast injection confirms the enhancing tumor is confined to the anterior vaginal wall, without definitive bladder invasion (*black arrow*) or rectal involvement (*white arrow*). *B* bladder, *T* tumor, *G* gel.

signal, depending on the amount of necrosis in the lymph node tissue. On non-fat-saturated T2-weighted images, the lymph nodes will be similar in intensity to the primary tumor, and stand out from the bright surrounding body fat (Fig. 4a). On T1-weighted post-contrast images, lymph nodes may be enlarged and have variable enhancement depending on the amount of necrosis in the lymph node (Fig. 4b). On DW images, metastatic lymph nodes are iso- to hyperintense on the lower B-value, become higher in signal on the higher B-value, and are dark on the apparent diffusion coefficient (ADC) map (Fig. 4c). Lymph node metastases have been shown to have significantly decreased ADC values when compared to benign lymph nodes, and abnormal nodes as small as 5 mm may be detected with DW imaging [35, 52]. However, some investigators have noted some metastatic lymph nodes will not exhibit restricted diffusion [21, 22, 34].

Table 2. 5-year survival comparison of women with and without positive lymph node metastasis

Lymph node status	5-year survival (%)
Negative lymph nodes	95
Positive pelvic lymph nodes	<80
Positive common iliac/para-aortic lymph nodes	<40

PET/CT in the assessment of cervical cancer: staging and treatment decision

PET/CT is utilized pre-treatment when there is potential for tumor spread beyond the cervix or in patients who are being considered for trachelectomy [13–15, 53]. The

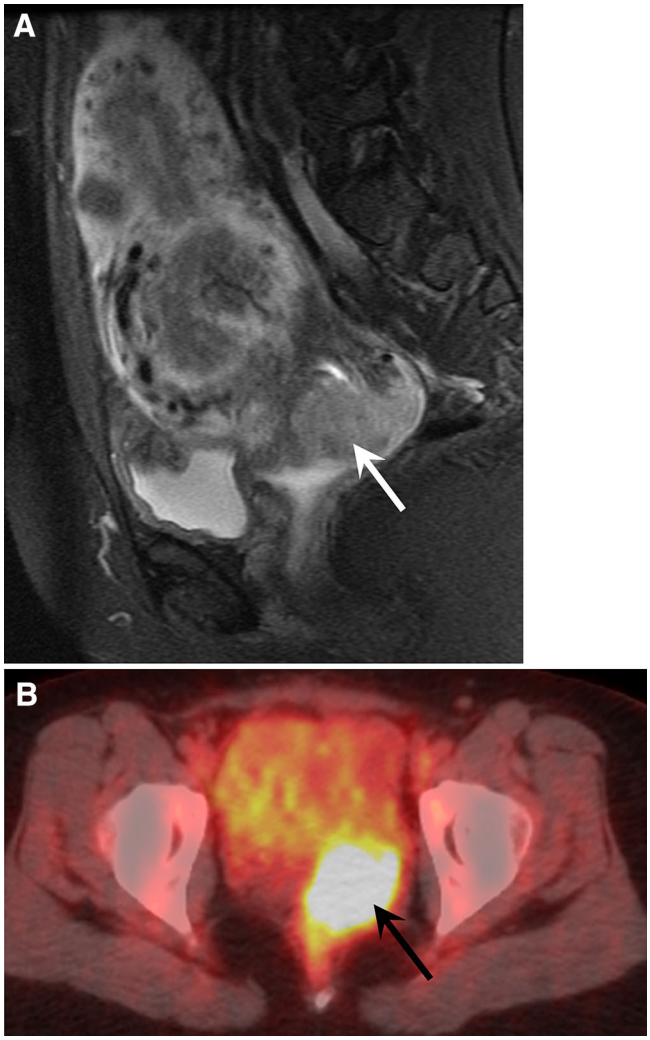

Fig. 6. 41-year-old female with small cell cervical cancer, stage IIIB clinically. **A** T2-weighted sagittal MR image demonstrates the primary tumor in the cervix (*white arrow*). **B** Axial fused PET/CT image demonstrates hypermetabolic activity on PET/CT (*black arrow*) in the area of the cervical cancer.

goals of PET/CT imaging are to assess the number and location of suspicious lymph nodes and to detect any metastatic soft tissue deposits [10, 13, 14, 32, 38, 54–56]. The reported PET sensitivity for lymph node detection ranges from 79% to 91%, and the specificity ranges from 93% to 100% [14, 37, 55, 56]. PET/CT has a potential advantage of incorporating the functional, metabolic PET data with the spatial resolution of CT; however, microscopic metastases may still be missed.

PET/CT plays a complementary role to MR imaging in the evaluation of local extent of disease and can be helpful in delineating the margins of an invasive tumor in cases of superior tumor extension into the uterine cavity and caudal extension into the vaginal cuff [7, 9, 13–15,

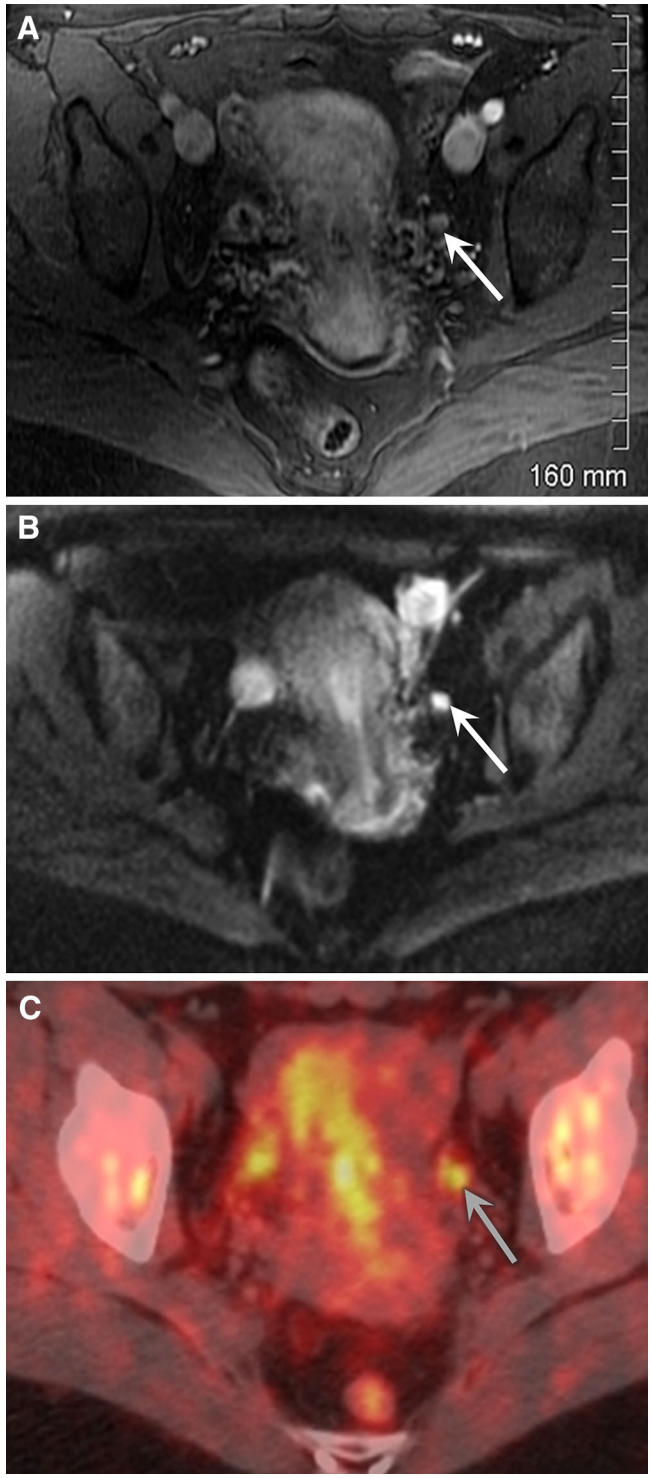

Fig. 7. 35-year-old female with clear cell cervical cancer, stage IB1 clinically. **A** T1-weighted post-contrast axial MR image reveals a small left external iliac node measuring 6 mm (*white arrow*). **B** The B = 500 image from the diffusion-weighed acquisition depicts the 6-mm lymph node (*white arrow*). On MRI this may be considered benign. **C** Axial fused PET/CT image demonstrates FDG uptake within the 6-mm lymph node seen on the corresponding MR images, rendering this lymph node suspicious (*gray arrow*).

Table 3. Example PET/CT scanning parameters for imaging patients with cervical cancer

PET/CT scanning parameters	
CT acquisition parameters	
Rotation time (s)	0.5
Detector coverage (mm)	40
Beam collimation (mm)	40
Detector rows	64
Pitch	0.516
Speed (mm/rotation)	20.62
Detector configuration	64 × 0.625
Slice thickness (mm)	5
Interval (mm)	3.27
kilovolts	140
Smart milliamps/auto milliamps range	60–500
Noise index	25
PET acquisition parameters	
Time/bed position	3 min
Matrix size	128 × 128
Reconstruction method	3D-iterative Vue point
Post filter (full width half maximum)	6
Loop filter (full width half maximum)	None
Display field-of-view (cm)	70
Number of iterations	2
Number of subsets	28

32, 34]. Although the primary tumor in the cervix will avidly uptake FDG and the tumor can be localized on PET/CT, the intense activity can exaggerate tumor extension into the parametrial tissues, as well as bladder and rectal involvement (Fig. 5). MR imaging should be used in conjunction with PET/CT to avoid overestimating local invasion into the parametrium, bladder, and rectum [21]. The reported sensitivity of MR imaging in the evaluation of bladder and rectal invasion is 71–100%, with a specificity of 88–91%, and a negative predictive value of MR imaging approaching 100% [24]. Therefore, invasive cystoscopic or endoscopic staging is no longer necessary and rarely used [8, 9, 24].

It is important to note that lymph node status is not part of the official FIGO 2009 staging system as lymph nodes cannot be determined on clinical examination. However, lymph node status is important in the treatment planning algorithm and an important predictor of outcome [5, 21, 23, 24, 27, 57]. Five-year survival for patients with early stage disease decreases from 95% in

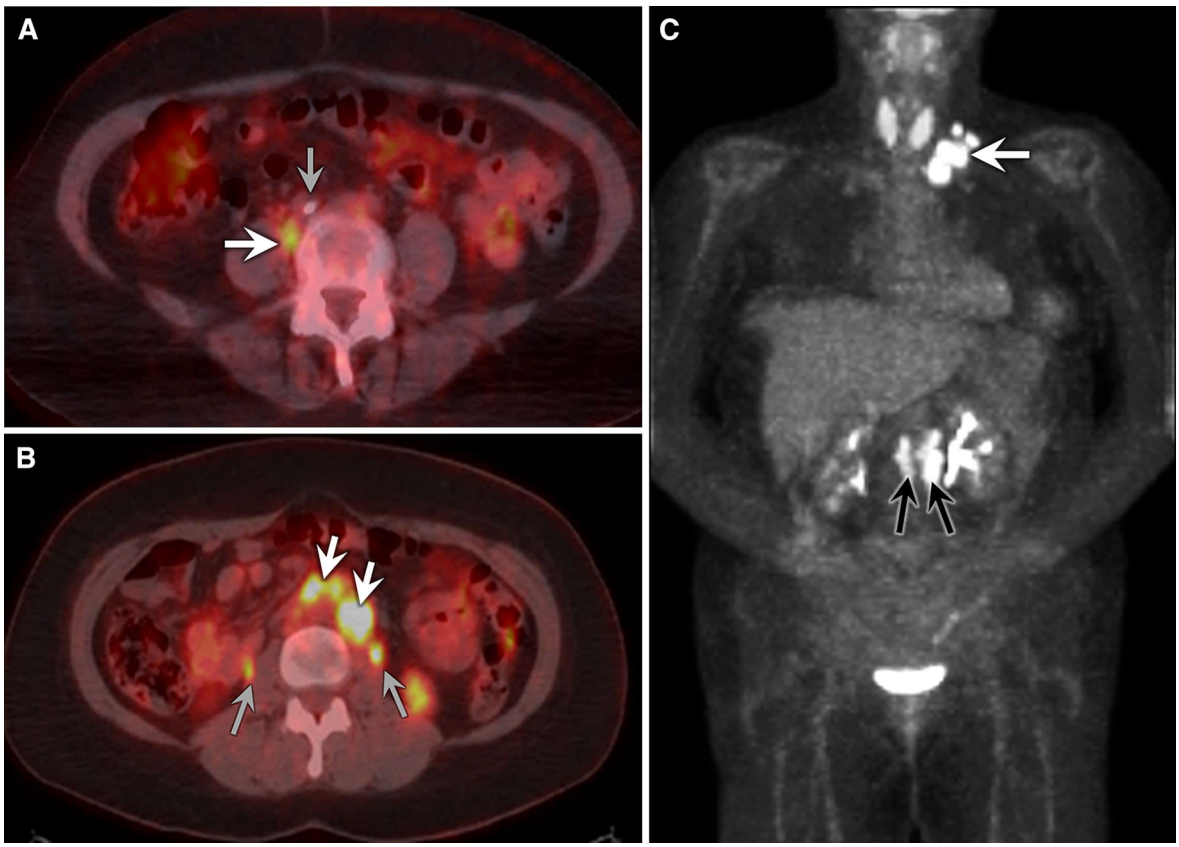

Fig. 8. 49-year-old female with clinical stage IV squamous cell cervical cancer. **A** Axial fused PET/CT images at the level of the common iliac vessels. Note there is a FGD avid lymph node (*white arrow*) along the right common iliac vessels, posterior and lateral to the right ureter (*gray arrow*). **B** Axial fused PET/CT images above the bifurcation of the aorta. Note there are multiple FGD avid lymph nodes (*white arrows*) in the para-aortic region. The ureters (*gray arrows*) are seen in this image as well, lateral and posterior to the retroperitoneal lymphadenopathy. **C** PET maximum intensity projection image depicting enlarged cervical lymph nodes (*white arrows*) in addition to the para-aortic lymphadenopathy (*black arrows*).

the absence of lymph node metastases to <80% if pelvic lymph node metastases are present and <40% % if there is metastasis to para-aortic lymph node (Table 2) [57].

PET/CT is also used to follow patients after radiation therapy to assess for treatment response and assess for recurrence in those with a complete response following initial treatment [13, 32, 58]. Overall, sensitivity and specificity of FDG-PET for detection of recurrent disease have been reported as 90% and 76%, respectively [49]. PET/CT, similar to MR imaging, is being assessed as a functional imaging parameter to predict disease response and prognosis, including disease-free and overall survival [5, 13, 46].

PET/CT protocol

In order to prepare for a PET/CT, the patient ideally should fast for 4–6 h prior to the examination. Small amounts of water with medications are acceptable. For diabetic patients, we recommend no insulin or oral hypoglycemic medications for 6 h prior to the radiotracer injection, and the blood glucose level prior to examination should be less than 200 mg/mL. The F-18 fluorodeoxyglucose dose is calculated as (weight in kg) × 0.14 mCi/kg with a minimum dose of 10 mCi. The uptake period spans at least 45 min, and the duration is recorded such that the uptake period can be held constant for subsequent studies in the same patient. During the uptake period, patients should be kept warm (warm blankets if necessary) and as relaxed as possible. Patients are instructed to minimize all movements and empty their bladder at the end of the uptake period. A routine field-of-view for patients with cervical cancer includes the thighs through the skull base. First, the scout scans are obtained, followed by low-dose non-contrast CT images, and finally the PET scan (Table 3). PET scan time may

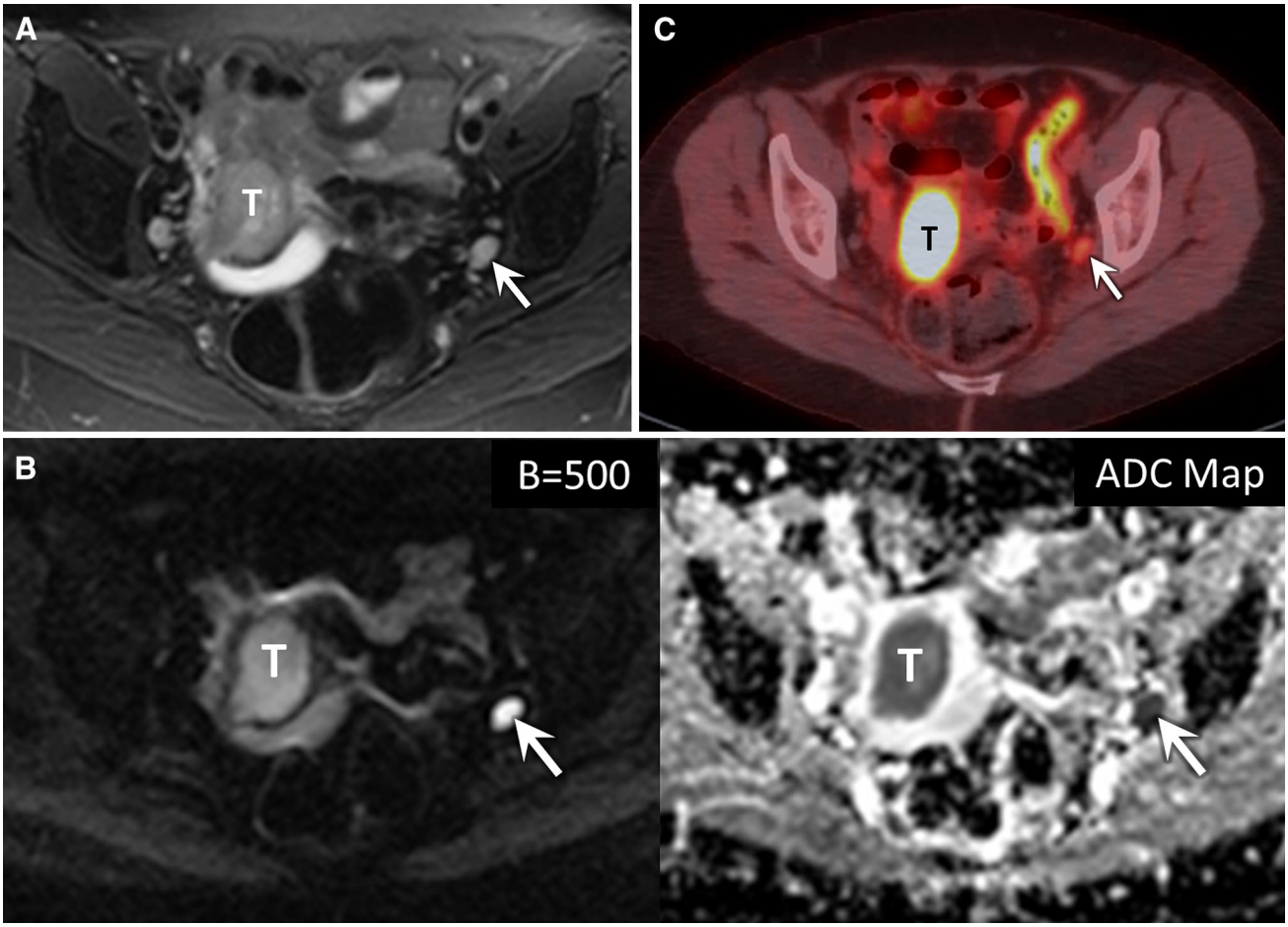

Fig. 9. 60-year-old female with cervical cancer, staged IB1 clinically. **A** On MRI, the axial T2-weighted image depicts an 8-mm lymph node along the left pelvic sidewall (*white arrow*). **B** The DW images depict the 8-mm lymph node as more hyperintense on the B = 500 image and dark on the ADC map (*white arrows*), signifying restricted diffusion. **C** Axial fused PET/CT images at the level of the 8-mm lymph node seen on the MRI demonstrates mild increased FDG uptake (*white arrow*). The lymph node was non-palpable on physical exam and clinically the patient had been staged as IB1. Because this was the only sizable lymph node found on imaging, and due to the restricted diffusion and FDG uptake, the treatment was changed from surgery to chemoradiation therapy. The primary tumor (T) is seen in the cervix.

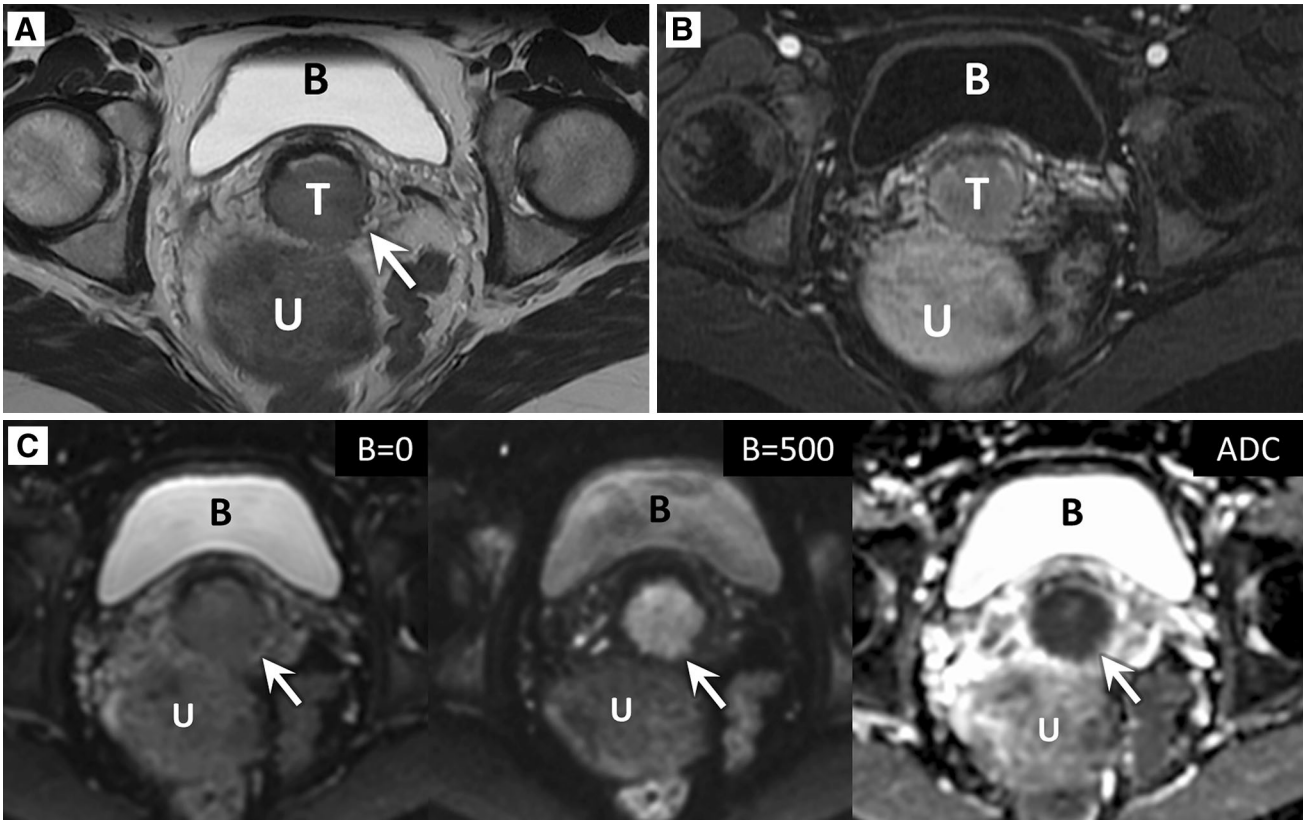

Fig. 10. 48-year-old female with clinically staged IB1 squamous cell carcinoma of the cervix. **A** Axial T2-weighted image depicts a 4 cm mass within the posterior cervix (T). There is minimal extension into the left parametrial soft tissues (*white arrow*). **B** Axial T1-weighted image post-contrast image with a mildly enhancing tumor seen in the cervix (T). **C** The DW images demonstrate the tumor as isointense on the B = 0 image, hyperintense on the B = 500 image, and dark on the ADC map (*white arrows*), signifying restricted diffusion. The parametrial extension of the cervical tumor was not palpable on physical exam, and clinically the patient had been staged as IB1. After the MR imaging examination, the patient was upstaged to stage IIB, and the treatment was changed from surgery to chemo-sensitized radiation.

be increased to optimize the image quality. Images are reviewed with the patient on the table and, if necessary, certain images may be repeated. All images are reconstructed with and without attenuation correction. Fused axial, sagittal and coronal, coronal PET/CT images, and maximum intensity projection (MIP) PET images are sent to the picture archiving and communication system (PACS).

PET/CT image analysis

Analysis of the images is performed on the workstations equipped with fusion imaging software. Initially, qualitative assessment for areas of increased metabolic uptake is performed based on provided images (Fig. 6). Semiquantitative measurements using maximum standardized uptake value (SUVmax) can be calculated by the following formula: SUVmax = tissue radioactivity concentration (mCi/mL)/(injected dose (mCi)/patient weight (g)). Because tumors demonstrate a range of increased metabolic activity with some of them being only mildly metabolic, strict cutoff SUVmax values for differentiating normal from abnormal uptake have not been established; however, values exceeding 2.5 are often considered suspicious when assessing for disease recurrence [59, 60]. On a pretherapy scan, SUV max has been noted as a prognostic factor for lymph node involvement, treatment response, and overall prognosis [54, 60]. At many institutions, small (<1 cm in short axis) lymph nodes are not considered worrisome on MR imaging; however, if there is hypermetabolic activity in the lymph node on PET, it is considered worrisome for metastasis (Fig. 7). In general,

caution has to be taken when evaluating small lesions (diameter of less than 2 times resolution of PET), because these lesions may demonstrate falsely decreased measured SUVmax values due to partial volume effect [61, 62]. For follow-up scans, SUVmax values for the primary lesion and metastatic lesions are reported with comparison to prior, with special attention paid to uptake time and any possible extravasation of the radiotracer, which could alter the calculated SUVmax values [61].

Fused PET/MR images in the assessment of cervical cancer: the future of cervical cancer imaging

The fusion of PET images with MR images is a new and emerging technology being used to evaluate cervical cancer patients. According to recent studies, the strengths of MR imaging in assessing local tumor extent, paired with the strengths of PET imaging in assessing lymph node metastasis, results in a synergistic effect on

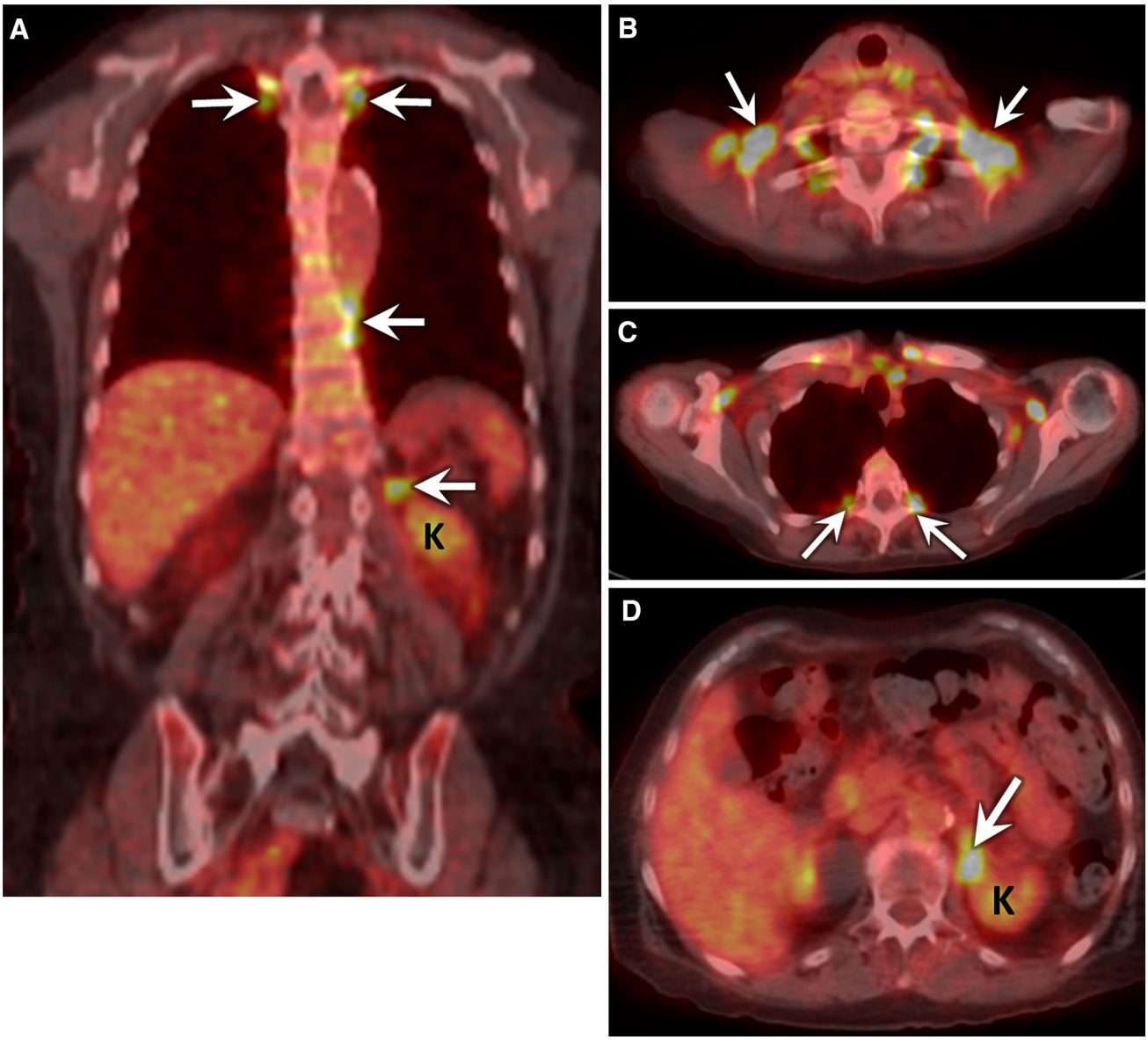

Fig. 11. 73-year-old female with stage IIIB squamous cell carcinoma of the cervix. **A** Fused coronal PET/CT image depicts multiple foci of hypermetabolic activity in regions of brown fat along the spine and above the left kidney (*white arrows*). No discrete lymph nodes or soft tissue, only fat was seen in these areas on the CT image. **B**–**D** Corresponding axial images demonstrate numerous foci of numerous hypermetabolic activity in fat in the supraclavicular, anterior mediastinal, axillary, peri-clavicular, paravertebral intercostal spaces and above the left kidney (*white arrows*). Because of the intense diffuse FDG activity in multiple regions of brown fat in this patient, the PET/CT was repeated with maneuvers to diminish the FDG uptake in brown fat. *K* kidneys.

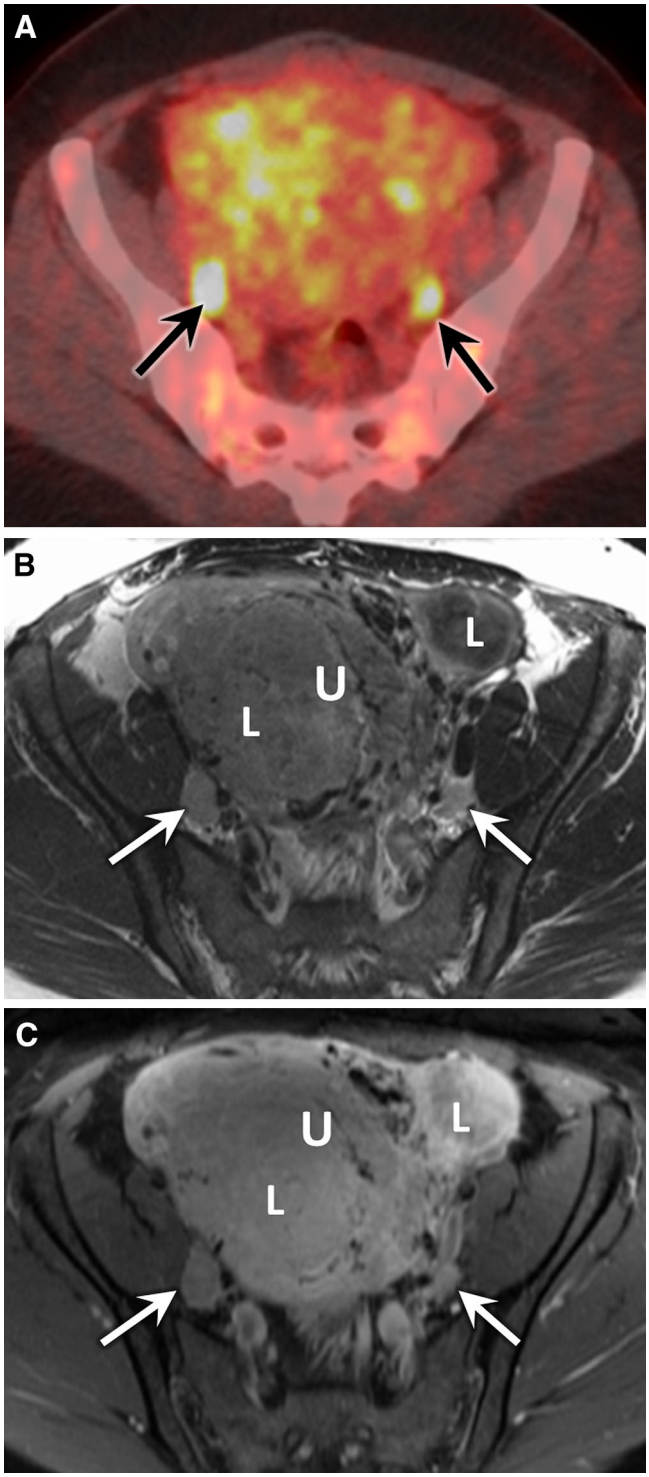

Fig. 12. 41-year-old female with stage IIIB cervical cancer. **A** Axial fused PET/CT image demonstrates two small symmetric foci of FDG uptake in the posterior pelvis, thought to represent physiologic ovarian activity (*black arrows*) when the PET/CT was first interpreted. **B** Axial T2-weighted MR image depicts bilateral abnormally enlarged pelvic lymph nodes consistent with metastases (*white arrows*), in the region of the FDG uptake on PET/CT. **C** Axial T1-weighted image post-contrast image demonstrates enlarged enhancing lymph nodes. The large enhancing structure in the mid and anterior pelvis is the uterus (*U*) with leiomyomas (*L*).

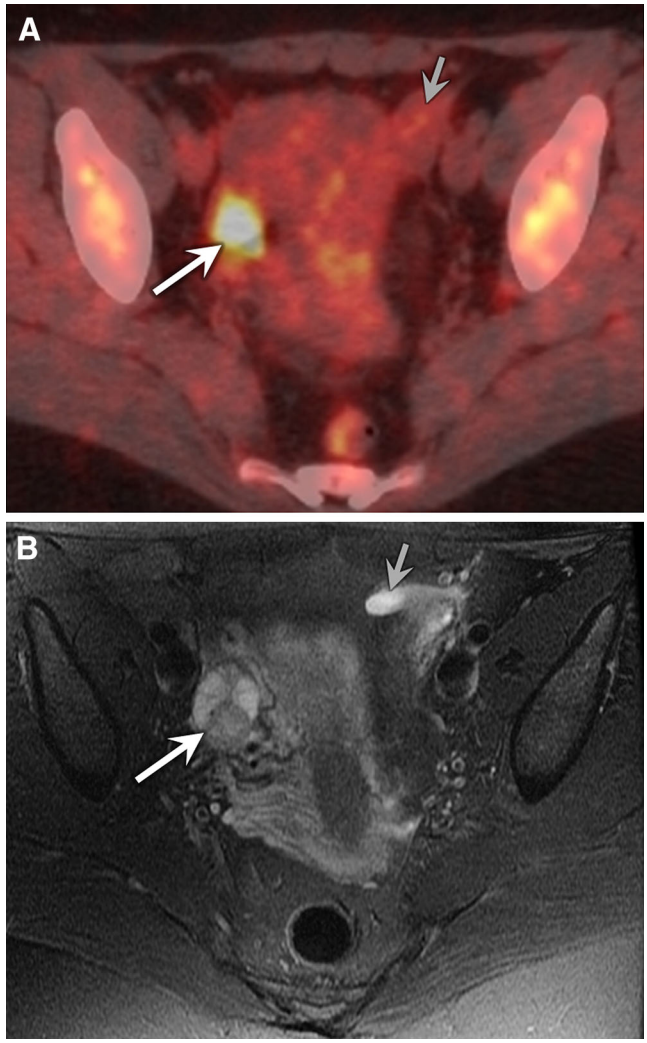

Fig. 13. 35-year-old female with clinically staged IB1 cervical cancer. **A** Axial fused PET/CT image demonstrates a focus of FGD uptake in the right pelvis, initially questioned as an enlarged pelvic lymph node versus a normal ovary (*white arrow*). **B** Axial T2-weighted MR image depicts a normal appearing ovary containing follicles, confirming the finding on PET/CT is a normal ovary (*white arrow*). Note the contralateral ovary (*gray arrow*) is not FDG avid.

the accuracy of staging women with cervical cancer [63, 64]. The accuracy of fused PET/MR was 83.3% for tumor staging and 90% for detection of lymph node metastasis, compared to an accuracy of 53.5% and 90%, respectively, for PET/CT [63]. Furthermore, readers detected more metastatic lymph nodes on fused MR/PET than they did on PET/CT in a group of 79 patients with cervical cancer who underwent lymphadenectomy as part of their cancer treatment [64]. Investigators have noted that fused PET/MR images combine the individual advantages of both modalities, which has resulted in its superior performance in reader studies. Certainly, future work in this area and the clinical utilization of PET/MR

scanners will increase the value of this new imaging technique in the staging and treatment of patients with cervical cancer.

Examples of PET/CT and MR imaging findings which affect treatment planning

Positive common iliac nodes, retroperitoneal nodes, or thoracic/cervical nodes

Lymph node status is an important prognostic factor and knowledge of extra-pelvic nodal involvement is critical for guiding the patient's treatment [32, 54, 65]. Locally advanced cervical cancer (tumors which extend beyond the cervix) places the patient at an increased likelihood of a positive lymph node [32, 52] (Fig. 8). Notably, cervical cancers have two potential drainage pathways based on the location of the tumor. Tumors which are located more caudally, in the cervix/lower uterine segment, usually drain first to the pelvic lymph nodes and subsequently into the common iliac chain. Tumors which extend further into the uterus than the lower uterine segment can potentially drain directly into the common iliac lymph nodes, bypassing the pelvic lymph node basin entirely [66]. The potential for common iliac nodal involvement without pelvic nodal involvement is an important reason to obtain a PET/CT in conjunction with MR imaging prior to treatment planning [8, 10, 15, 57]. When imaging reveals suspicious common iliac and paraaortic lymph nodes, the radiation field must be expanded to include these regions. The presence of suspicious thoracic or cervical lymph nodes alters management as these patients are typically managed with palliative intent, rather than potentially curative surgery or chemoradiotherapy.

Positive pelvic lymph nodes in clinically early stage tumors

Early stage cervical cancers which are small (<4 cm) and confined to the cervix have a very low rate of lymph node metastasis. This is true in both low-risk histology cell types (squamous cell) and higher risk cell types (small cell carcinoma, adenosquamous carcinoma, mucinous carcinoma, and clear cell carcinoma) [67]. MR imaging and PET/CT can assess for unexpected lymph node spread prior to treatment planning (Fig. 9). The presence of positive lymph nodes increases the likelihood of recurrence and decreases the survival rate compared to women without lymph node metastasis [57]. From a treatment planning perspective, women with imaging positive lymph nodes are not considered surgical candidates, and chemoradiotherapy is recommended [67, 68].

Parametrial invasion

Parametrial invasion is sometimes difficult to appreciate clinically, and occasionally clinically Stage I and IIA tumors demonstrate parametrial invasion on MR imaging (Fig. 10). This upstages the patient to at least Stage IIB and changes the treatment from surgery to chemoradiation therapy. The reported sensitivities of MR imaging for detecting parametrial involvement of cervical cancer are greater than 90%, with specificities greater than 80% and negative predictive values as high as 94–100% with modern MR imaging sequences [21, 22, 27, 28]. However, in large tumors, MR imaging may overestimate parametrial invasion when compared with small tumors as a result of stromal edema caused by tumor compression or inflammation [24, 25]. Review of DW images may be helpful to avoid overestimating parametrial invasion. On PET/CT, the extent of hypermetabolic activity in the primary tumor can overestimate parametrial invasion. Overestimation of parametrial invasion on PET/CT is mainly due to the lower resolution of PET images, and MR images should be used to assess parametrial invasion more accurately [13, 15, 69].

PET/CT pitfalls: biodistribution and benign lesions

Biodistribution pitfalls: brown fat

An interpreting radiologists or nuclear medicine physician should be aware of potential pitfalls in PET/CT evaluation. One PET/CT pitfall frequently encountered is metabolic activity within brown fat on the PET images [70]. Brown fat activity can be relatively easily discerned from pathologic hypermetabolic activity by observing the distribution pattern and correlating with the CT. On CT, there will be fat without lymph nodes in the regions of FDG uptake (Fig. 11). At our institution, warm blankets are routinely used to prevent this phenomenon from happening. Additional measures, such as propranolol and/or anxiolytics, are used in selected cases. If there are no contraindications to beta blockers, one of the protocols used in our institution includes 20 mg of Propranolol orally 60 min prior to the FDG injection.

Biodistribution pitfall: physiologic metabolic activity in ovaries and endometrium

Increased FDG uptake in the ovaries and endometrium can be seen at various points during the menstrual cycle [71]. Unilateral or bilateral ovarian FDG uptake may be seen in pre-menopausal female patients during follicular development, but in some women it can be seen throughout the menstrual cycle. Any FDG activity in the uterus and adnexa should correlate with the anatomical

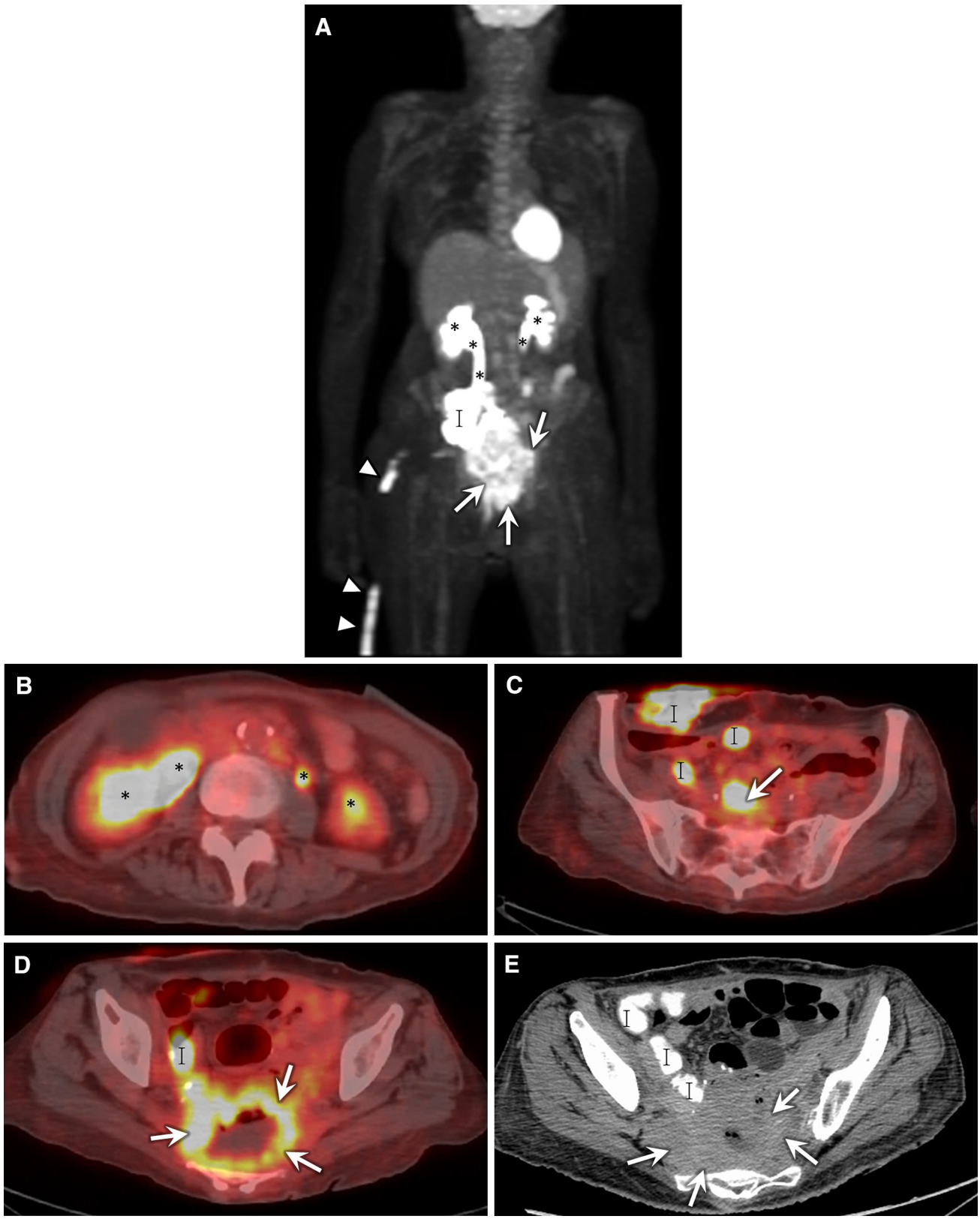
A
B
C
D
E

◀ **Fig. 14.** 66-year-old female with stage IB2 squamous cell cancer of the cervix. **A** Coronal PET image reveals dilated ureters and collecting systems bilaterally, *right* greater than *left* (*black asterisks*). There is a large amount of FDG activity in the right mid pelvis, some of which is within the patient's known ileal conduit (*I*). The remainder of the activity was initially questioned as a urinary leak (*white arrows*). External urinary tubing noted (*arrowheads*). **B–D** Axial fused PET/CT image depicts hypermetabolic fluid in the collecting system of the kidneys (*black asterisks*), ureters (*black asterisks*), and ileal conduit (*I*). There is a lobular ring-like collection of FDG activity deep and posterior to the ileal conduit, which was a questioned urine leak (*white arrows*). **E** Axial CT image at 40 min post-contrast injection, from a CT obtained on the same day as the PET/CT, reveals a rim of soft tissue in the pelvis (*white arrows*), below the level of the ileal conduit (*I*), which was clinically unexpected recurrent metastatic disease.

structures on MR images. Care must be taken not to mistake uptake in bilateral pathologic lymph nodes as normal ovaries (Fig. 12). On the other end of the spectrum, mistakenly diagnosing metastatic disease when normal ovaries account for the FDG uptake can be avoided by identifying an ovary containing small follicles and dark stroma on the T2-weighted MR images (Fig. 13). Another potential pitfall is related to ovarian transposition, which is performed in young patients in order to protect the ovary from radiation therapy. A transposed ovary is placed above the pelvic brim and can be easily mistaken as an abdominal metastasis if the possibility of transposition is not kept in mind [72].

Biodistribution pitfall: urine activity

PET interpreters are well aware of high physiologic urine activity due to urinary excretion of the FDG [71]. Potential false-positive and false-negative results may occur due to focal urinary retention of FDG in a ureter, bladder diverticulum, pelvic kidney, and surgically constructed ileal conduit or neobladder [47]. In patients with a neobladder or ileal conduit, special care must be taken to ensure that all FDG activity is contained within these structures, so that a recurrence or pelvic metastasis is not missed. For example, in Fig. 14, a patient with a known ileal conduit for urinary diversion was seen to have "lobular" FDG uptake in the region below the expected ileal conduit, and a urine leak was suspected on the PET/CT examination. However, when the contrast-enhanced CT images were scrutinized, soft tissue due to tumor recurrence, rather than fluid, was found in the area of suspected urine leak.

Biodistribution pitfall: bowel activity

Bowel activity can be highly variable on PET and can be diffuse or focal in appearance. As with urinary activity,

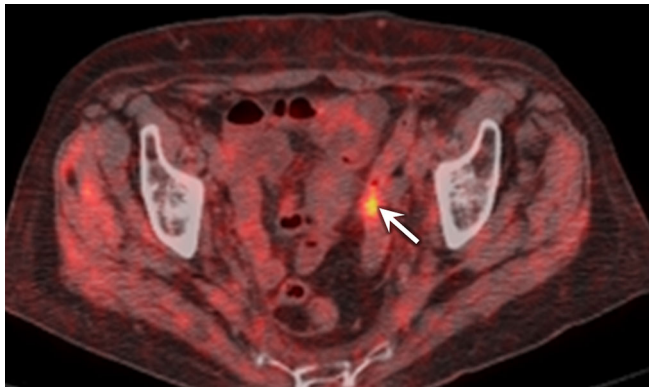

Fig. 15. 49-year-old women with stage IB1 squamous cell cervical cancer. Axial fused PET/CT image demonstrates very focal intense FDG uptake in the sigmoid colon (*white arrow*). Colonoscopy was performed, which revealed a polyp. This was removed at the same time, and pathology was consistent with a pre-cancerous adenomatous polyp.

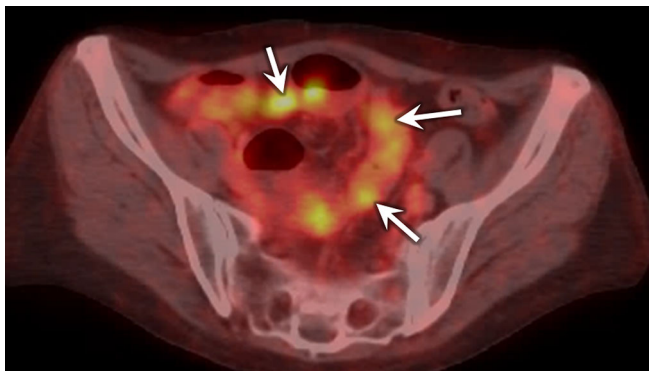

Fig. 16. 43-year-old women with stage IIB squamous cell cervical cancer. Axial fused PET/CT image demonstrates focal diffuse FDG uptake in the sigmoid colon (*white arrow*). The patient was near the end of her radiation treatments and was experiencing diarrhea and abdominal pain. Correlation between the imaging findings and symptoms lead to the clinical diagnosed of radiation colitis. This was treated conservatively with resolution of symptoms a few months after cessation of the radiation treatments.

disease may be over- or underestimated. If there is very focal activity confined to a small segment of colon, correlation with CT for a mass or evaluation with CT colonography or optical colonoscopy can be performed [73, 74]. This was the case in Fig. 15 in a patient where a very focal area of intense FDG uptake was noted in the sigmoid colon, with relatively less FDG uptake in the remainder of the bowel. The patient was referred to colonoscopy, and a pre-cancerous adenomatous polyp was removed.

More diffuse or segmental FDG uptake is often normal. However, when there is relatively more FDG

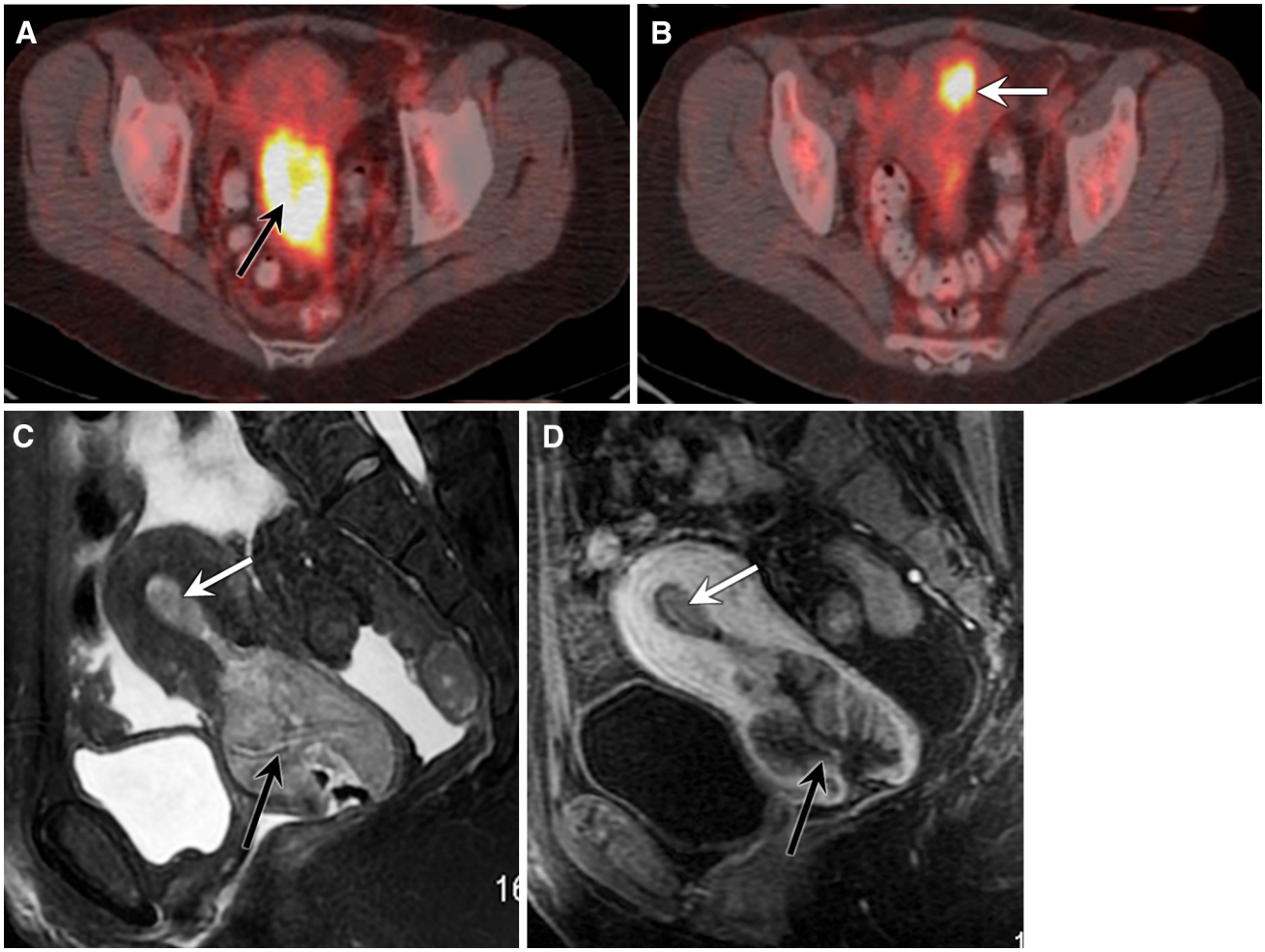

Fig. 17. 48-year-old female with high-grade invasive cervical cancer. **A** Axial PET/CT fused image at the level of the cervical cancer (*black arrow*). **B** Axial PET/CT fused image at the level of the uterus with a round focus of FDG uptake in the center of the uterus (*white arrow*). **C** Sagittal T2-weighted MR image depicts the cervical tumor in the cervix (*black arrow*) and abnormal signal in the endometrial canal (*white arrow*) at the level of the round focus of FDG uptake on the PET/CT fused image. No leiomyomas are present on this image or the remainder of the uterus. **D** Sagittal T1-weighted image post-contrast image depicts contrast enhancement of the cervical tumor (*black arrow*) and enhancement of a tumor in the endometrial canal (*white arrow*).

activity in a long segment of bowel relative to the remainder of the bowel, this should be correlated with history and presence of pain or bloating. Occasionally inflammatory conditions, particular post-radiation enterocolitis occur in patients with cervical cancer (Fig. 16).

Benign lesions: leiomyomas

Leiomyomas are very common and can be hypermetabolic on PET imaging. Care should be taken to assure FDG avid foci in the uterus are truly leiomyomas on the corresponding MR images, so not to miss multifocal cervical cancer (Fig. 17). On MR imaging, leiomyomas are well-defined, hypointense on T2-weighted images, and can contain associated large serpiginous flow voids on T2-weighted images, in contrast to cervical tumor which is isointense on T2-weighted images and do not contain large flow voids. Larger, degenerating leiomyomas may have an area of high signal on T2-weighted images (Fig. 18). Both leiomyomas and cervical cancer will enhance following contrast, sometimes heterogeneously. DW images may be helpful to differentiate leiomyomas from tumor, as cervical cancer will restrict diffusion, while most leiomyomas will not. However, occasionally leiomyomas do restrict diffusion and the T2-weighted appearance should be relied upon to confirm the presence of a leiomyoma [75, 76].

Benign lesions: Incidental inflammatory/infectious lesions

Infectious and inflammatory processes result in FDG uptake; therefore, it is critical to consider the clinical picture to avoid misdiagnosing a neoplasm. Physical examination may also be of benefit in certain circumstances particularly for hypermetabolic lesions in the skin, mucosal pharyngeal space, or rectum. An example of the need to clinically correlate with physical examination is presented in Fig. 19. In this case, there was significant FDG uptake in the rectum, and recurrence in this region was questioned based on the PET/CT images. Corresponding MR images of this region demonstrated only normal anatomical structures. Ultimately, physical examination was performed and an inflamed hemorrhoid was present accounting for the FDG uptake on the PET/CT examination.

PET/CT pitfalls: post-radiation inflammation

Local inflammation secondary to radiation

Post-therapy findings can often be challenging on imaging. In the setting of cervical cancer, there are often post-radiation changes in the region of the primary tumor [15, 59]. In order to decrease false-positive results, PET is often delayed for 8–12 weeks after the completion of radiation therapy to allow for the inflammatory response to subside [72]. However, increased metabolic activity due to residual inflammation may be seen on PET several months post-radiation and often poses a diagnostic dilemma. Biopsy may ultimately be required if the imaging remains indeterminate. Such was the case in Fig. 20, which depicts an area of persistent FDG uptake in the cervix in a patient with cervical cancer, many months after completion of radiation therapy. MR imaging did reveal an area "suspicious" for tumor. This patient was referred to biopsy for the findings on imaging, which only revealed necrotic tissue and inflammatory fibrosis. On a follow-up PET/CT 1 year later, the FDG uptake in the cervix resolved.

Osseous activity

Following radiation, bone marrow activity may be increased or decreased, focally or diffusely [77]. In the early post-radiation period, there may be increased FDG uptake matching the radiation port due to inflammatory changes in the region of treatment. Following chemotherapy, PET/CT examination may also reveal diffusely increased bone marrow activity ("stimulation"), which is most commonly seen in patients treated with colony stimulating factors for leukopenia. Decreased activity within the radiation port is usually delayed and less worrisome. This reflects functional suppression of the bone marrow due to its high sensitivity to radiation therapy.

In addition to radiation-induced changes in the bone marrow, pelvic radiation therapy for cervical cancer places the patient at increased risk for developing osteoporosis and insufficiency pelvic fractures. Both radio-osteonecrosis and insufficiency fracture can present either early or late and may be difficult to differentiate from recurrent/metastatic disease due to variable degrees of FDG uptake [72, 77, 78]. Typically, insufficiency fractures develop in the sacrum, pubic rami, or acetabulum [79]. In certain cases, serial follow-up exams or further evaluation with MR imaging may be necessary to definitively differentiate benign from malignant processes (Fig. 21).

MR imaging pitfalls

Limited visualization of lesions outside the pelvis

PET/CT is superior to MR imaging in evaluating for distant metastatic disease. PET should be used to avoid missing lesions on the edges of the field-of-view on MR imaging. In addition, scout MR images should be carefully scrutinized for any abnormalities. An example of the value of evaluating all imaging sequences, including the localizer images, is given in Fig. 22. In this case, there was an inconspicuous metastatic soft tissue lesion in the anterior left abdominal wall overlooked on the MR imaging examination. The FDG avid soft tissue metastasis was seen on the PET/CT examination, and in retrospect, this lesion was only visible on the localizer MR images.

MR imaging suspicious lesions may not be metabolically active on PET-CT

Not all suspicious lesions detected on MR necessarily represent active metastatic disease. If the lesion is not metabolically active on PET, an alternative diagnosis must be sought. For instance, indolent infectious or inflammatory processes may occur in patients treated with radiation therapy. Such was the case in Fig. 23, where there were new bone lesions in the right superior pubic ramus on the MR images in a patient one year after completion of chemoradiation therapy. Corresponding PET/CT images reveal no FDG uptake in the bone lesion. After further clinical work-up, these were diagnosed as indolent osteomyelitis. Eventually, these did progress to a more aggressive infection which involved the pelvic musculature and abscesses formation.

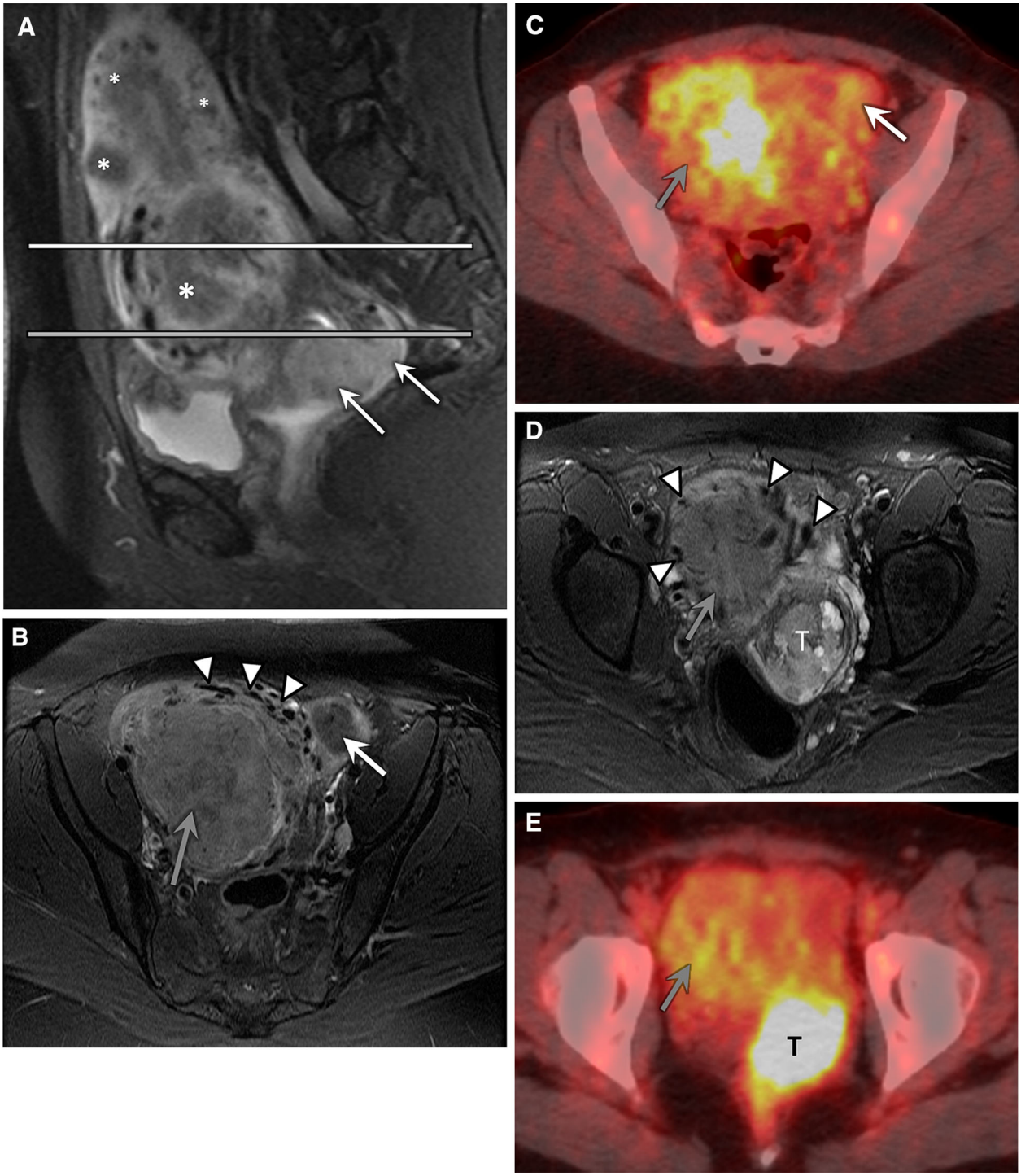
A
B
C
D
T
E
T

◀ **Fig. 18.** 41-year-old female with stage III B cervical cancer. **A** Sagittal T2-weighted MR image demonstrates multiple leiomyomas which appear as well-defined, round, hypointense lesions of varying sizes in the mid-body and fundus of the uterus (*white asterisks*). The cervical cancer involves both the anterior and posterior lip of the cervix (*white arrows*). The white and gray horizontal lines indicate two different levels on corresponding axial MR and fused PET/CT images in figure components **B**–**E**. **B** Axial T2-weighted MR image depicts two leiomyomas at the level of the white line in **A**. The left subserosal leiomyoma appears homogenously hypointense (*white arrow*), and the larger degenerating myometrial leiomyoma is more heterogeneously hypointense with areas of high signal (*gray arrow*). Multiple serpiginous flow voids (*arrowheads*) are noted in association with the larger leiomyoma. **C** Axial fused PET/CT image demonstrates mild FDG uptake in the smaller subserosal leiomyoma (*white arrow*) and more intense uptake in the larger degenerating myometrial leiomyoma (*gray arrow*). **D** Axial T2-weighted MR image at the level of the gray line in **A** depicts the most inferior extent of the larger myometrial leiomyoma (*gray arrow*) with a few associated flow voids (*arrowheads*) and the cervical cancer in the center of the cervix (*T*). **E** Axial fused PET/CT image demonstrates mild diffuse FDG uptake in the larger myometrial leiomyoma (*gray arrow*) and focal intense FDG uptake in the cervical cancer in the center of the cervix (*T*).

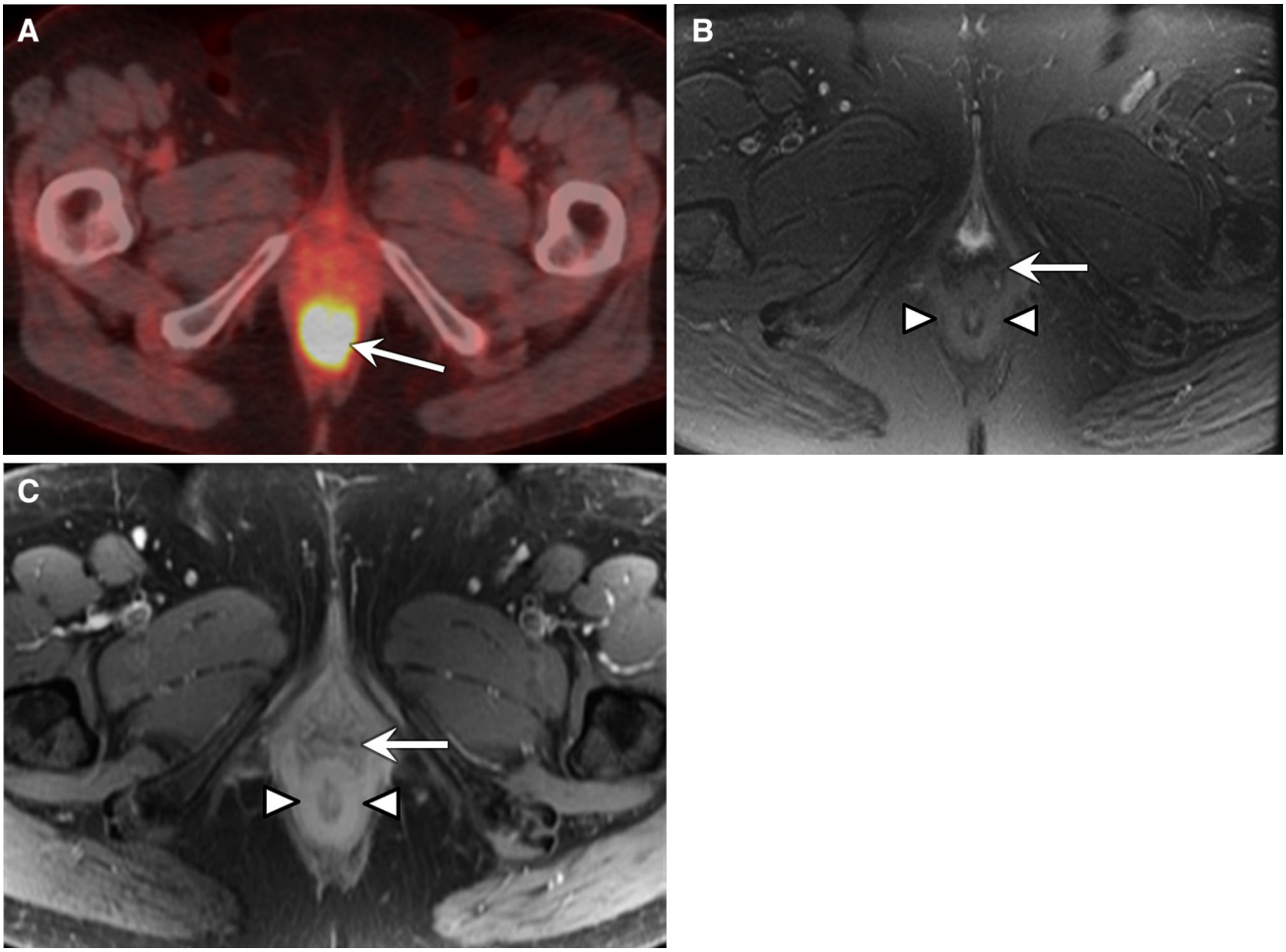

Fig. 19. 55-year-old female with stage IIB cervical cancer. **A** Axial PET/CT fused image demonstrates intense focal FDG uptake in the midline at the level of the inferior vaginal canal (*white arrow*). **B** Corresponding axial T2-weighted MR image depicts normal pelvic anatomy at the level of the FDG uptake, with no evidence of a mass in the distal rectum/anal canal (*arrowheads*) or vagina (*white arrow*). **C** Axial T1-weighted image post-contrast image also demonstrates only normal anatomical structures in the region of the FDG uptake. On physical examination, inflamed hemorrhoids were discovered, which accounted for the FDG uptake seen on the PET/CT image.

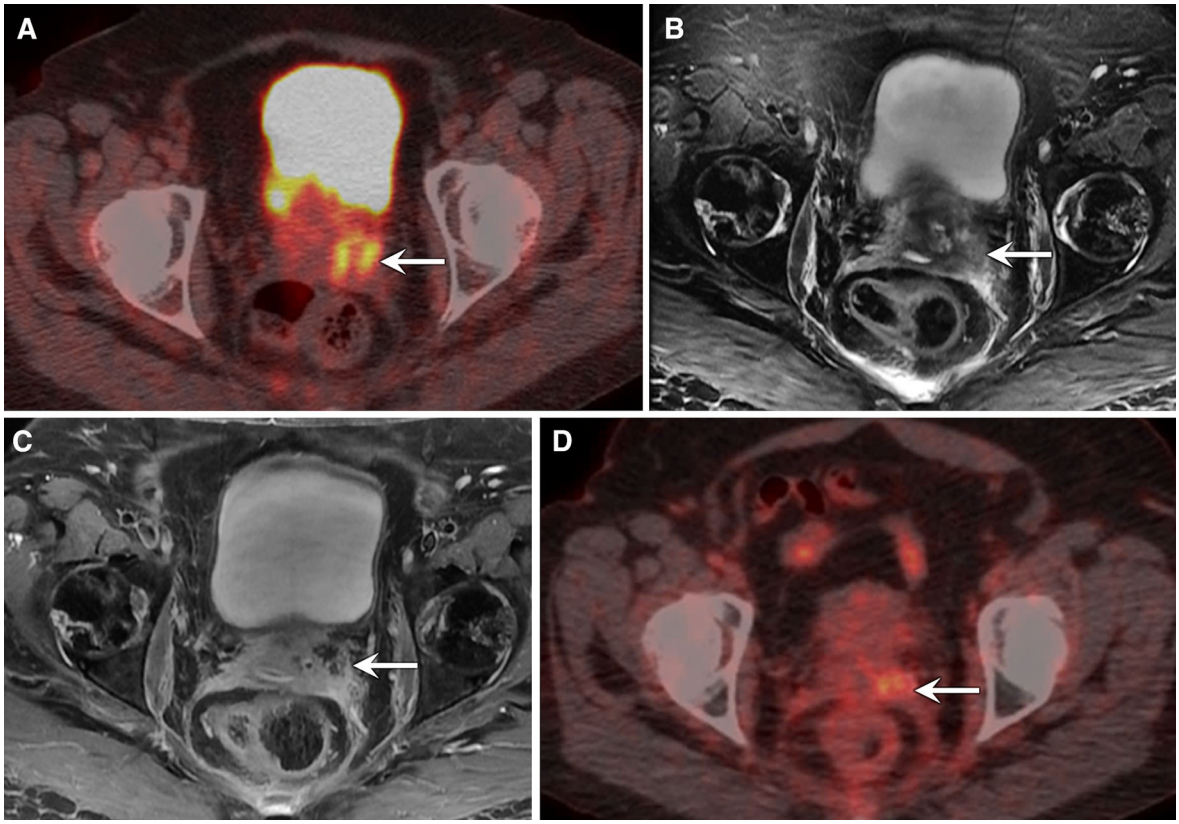

Fig. 20. 55-year-old female with stage IIB cervical cancer, 6 months post-radiation therapy. **A** Axial PET/CT fused image demonstrates focal FDG uptake in the region of the cervix (*white arrow*). **B** Axial T2-weighted MR image reveals a round ill-defined area of isointense signal, concerning for soft tissue along the left aspect of the cervix (*white arrow*). **C** Axial T1-weighted image post-contrast image demonstrates an enhancing lesion along the left aspect of the cervix, with an area of central non-enhancement suggesting necrosis. Overall, the imaging findings were concerning for residual disease. A biopsy was performed revealing only inflammatory cells. **D** Follow-up PET/CT examination a year later demonstrates almost complete resolution of hypermetabolic activity (*white arrow*).

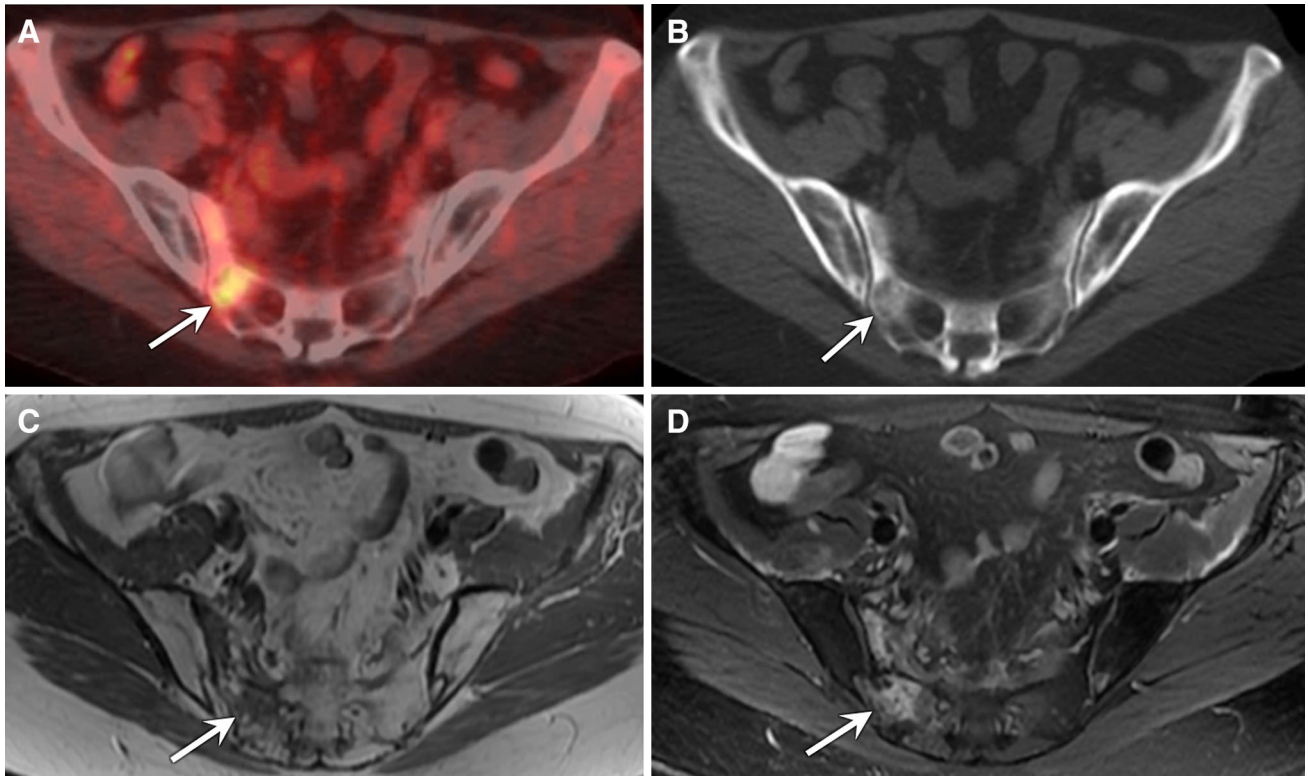

Fig. 21. 45-year-old female with stage IIB cervical cancer, being evaluated for recurrence. **A** Fused PET/CT image demonstrates an area of FDG uptake in the right sacrum (*white arrow*). **B** Corresponding axial CT image reveals a mixed sclerotic/lytic lesion in the area of FDG uptake (*white arrow*). **C** On the T1-weighted MR image from the same day, there is low signal in the region of the FDG uptake, with intermixed areas of fat (*white arrow*). **D** T2-weighted MR image reveals edema in the right sacral ala (*white arrow*). These imaging findings are most in keeping with radiation osteonecrosis.

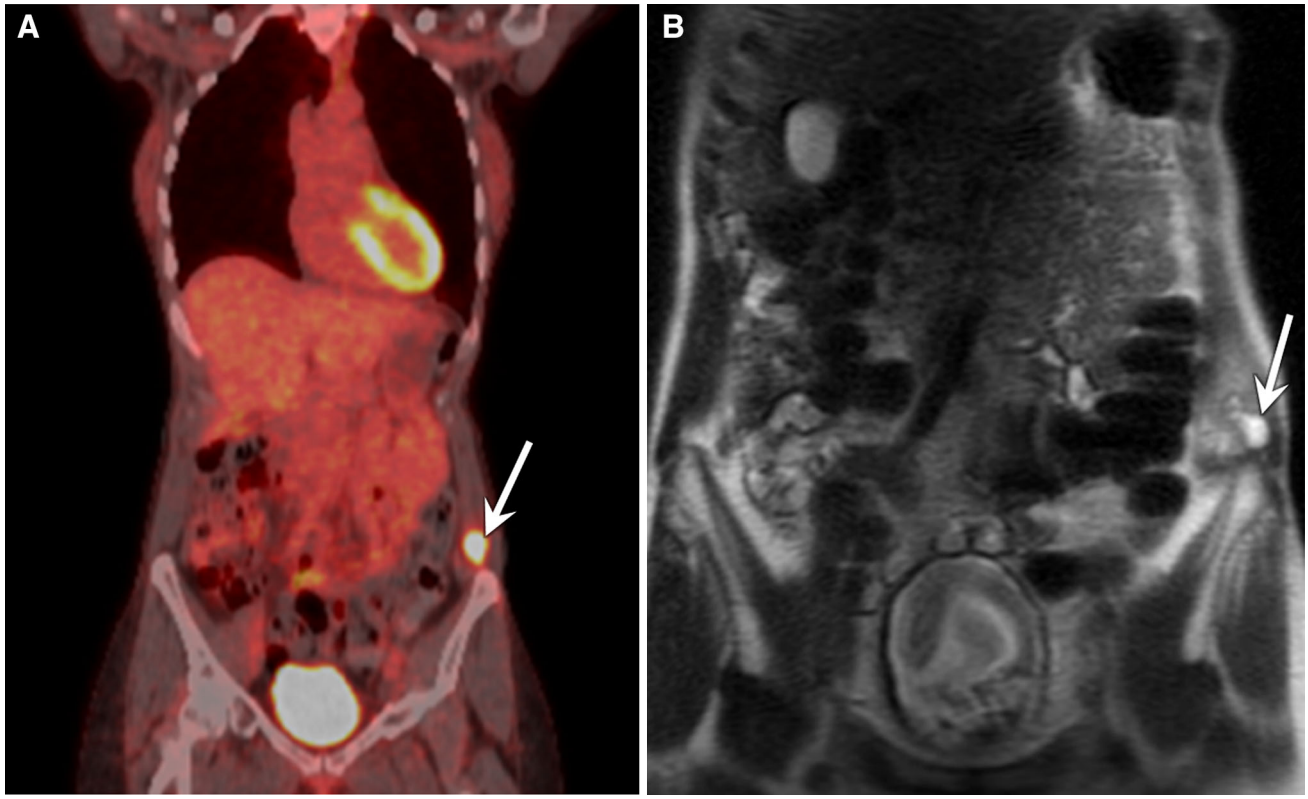

Fig. 22. 51-year-old female with recurrent squamous cell cervical cancer. **A** Coronal fused PET/CT image demonstrates an obvious focus of hypermetabolism (*white arrow*) in the left lower abdominal wall. **B** Coronal single shot fast spin echo localizer image depicts a cystic appearing lesion in the left lower abdominal wall (*white arrow*). This lesion was only seen on the localizer images and was discovered in retrospect (*white arrow*). A biopsy was performed revealing recurrent metastatic cervical cancer.

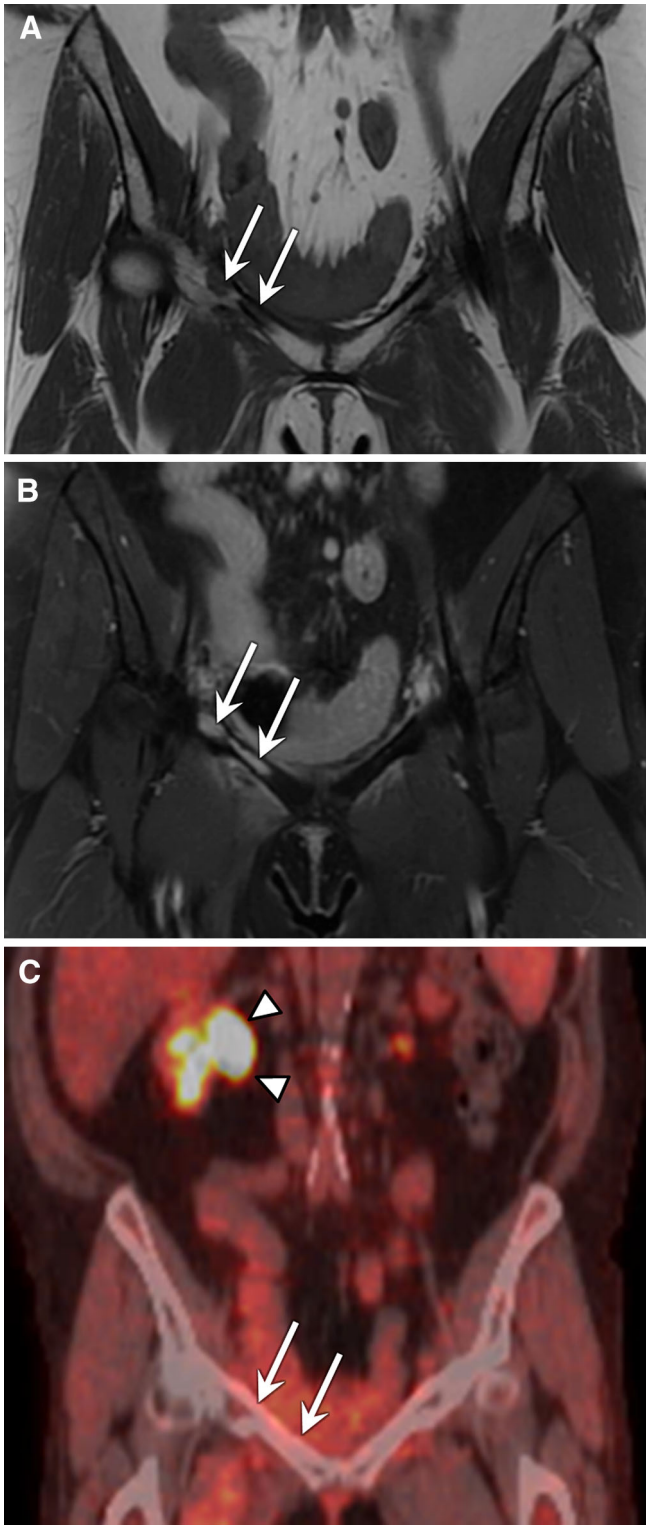

◀ **Fig. 23.** 42-year-old female 12 months post-radiation treatment for stage IIB cervical cancer. **A** Coronal T1-weighted MR image depicts new foci of low signal in the right superior pubic ramus (*white arrows*). **B** On the coronal T1-weighted image post-contrast image, the new foci in the right superior pubic ramus demonstrate avid enhancement (*white arrows*). **C** Corresponding coronal fused PET/CT image does not show any FDG uptake in the left pubic ramus (*white arrows*). Note the FDG activity in the collecting system of the left kidney for comparison (*arrowheads*). Ultimately, these lesions were foci of indolent osteomyelitis, which eventually progressed and the pelvic musculature became involved with infection and abscess formation.

Conclusion

The diagnosis, management, and follow-up of cervical cancer have evolved to include MR imaging and PET/CT in regions of the world where these advanced imaging modalities are available. The information gained from imaging guides and at times alters the course of treatment a patient undergoes. Imaging is also used in the follow-up of cervical cancer patients to detect recurrence and determine the next line of treatment. Using contemporary imaging protocols and understanding the role MR imaging and PET/CT play in guiding management, as well as the potential pitfalls of these modalities, is imperative for the radiologist to render an interpretation that will assist the referring clinician as they formulate an optimal treatment plan for the patient.

Conflict of interest. The authors declare that they have no conflict of interest.

References

1. Cancer Research UK (2012) Cervical cancer incidence statistics. http://info.cancerresearchuk.org/cancerstats/types/cervix/incidence/. Accessed 17 Aug 2014
2. http://www.worldlifeexpectancy.com/usa-cause-of-death-by-age-and-gender. Accessed 17 Aug 2014
3. International Agency for Research on Cancer (2013) WHO Press Release 12 Dec 2013. http://www.iarc.fr/en/media-centre/pr/2013/pdfs/pr223_E.pdf. Accessed 17 Aug 2014
4. Lea JS, Lin KS (2012) Cervical cancer. Obstet Gynecol Clin N Am 39:233–253
5. Barwick TD, Taylor A, Rockall A (2013) Functional Imaging to predict tumor response in locally advanced cervical cancer. Curr Oncol Rep 15:549–558
6. Green JA, Kirwan JM, Tierney JF, et al. (2001) Survival and recurrence after concomitant chemotherapy and radiotherapy for cancer of the uterine cervix: a systematic review and meta-analysis. Lancet 358:781–786
7. Grigsby PW (2007) The contribution of new imaging techniques in staging cervical cancer. Gynecol Oncol 107:S10–S12

8. Amendola MA, Hricak H, Mitchell DG, et al. (2005) Utilization of diagnostic studies in the pretreatment evaluation of invasive cervical cancer in the United States: results of intergroup protocol ACRIN 6651/GOG 183. J of Clin Oncol 23:7454–7459
9. Mitchell DG, Snyder B, Coakley F, et al. (2006) Early invasive cervical cancer: tumor delineation by magnetic resonance imaging, computed tomography, and clinical examination, verified by pathologic results, in the ACRIN 6651/GOG 183 intergroup study. J Clin Oncol 24:5687–5694
10. Chung HH, Kang KW, Cho JY, et al. (2010) Role of magnetic resonance imaging and positron emission tomography/computed tomography in preoperative lymph node detection of uterine cervical cancer. Am J Obstet Gynecol 203:156e1-5
11. Hricak H, Gatsonis C, Chi DS, et al. (2005) Role of imaging in pretreatment evaluation of early invasive cervical cancer: results of the intergroup study. J Clin Oncol 23:9329–9337
12. Narayan K (2005) Arguments for a magnetic resonance imaging-assisted FIGO staging system for cervical cancer. Int J Gynecol Cancer 15:573–582
13. Patel CN, Nazir SA, Khan Z, Gleeson FV, Bradley KM (2011) 18F-FDG PET/CT of cervical carcinoma. Am J Roentgenol 196:1225–1233
14. Havrilesky LJ, Kulasingam SL, Matchar DB, Myers ER (2005) FDG-PET for management of cervical and ovarian cancer. Gynecol Oncol 97:183–191
15. Rockall AG, Cross S, Flanagan S, Moore E, Avril N (2012) The role of FDG-PET/CT in gynaecological cancers. Cancer Imaging 12:49–65
16. Landoni F, Maneo A, Colombo A, et al. (1997) Randomised study of radical surgery versus radiotherapy for stage Ib-IIa cervical cancer. Lancet 350:535–540
17. Peters WA 3rd, Liu PY, Barrett RJ 2nd, et al. (2000) Concurrent chemotherapy and pelvic radiation therapy compared with pelvic radiation therapy alone as adjuvant therapy after radical surgery in high-risk early-stage cancer of the cervix. J Clin Oncol 18:1606–1613
18. Sedlis A, Bundy BN, Rotman MZ, et al. (1999) A randomized trial of pelvic radiation therapy versus no further therapy in selected patients with stage IB carcinoma of the cervix after radical hysterectomy and pelvic lymphadenectomy: A Gynecologic Oncology Group Study. Gynecol Oncol 73:177–183
19. Pecorelli S, Zigliani L, Odicino F (2009) Revised FIGO staging for carcinoma of the cervix. International Journal of Gynecology and Obstetrics 105:107–108
20. Pecorelli S (2009) Revised FIGO staging for carcinoma of the vulva, cervix, and endometrium. Int J Gynaecol Obstet 105:103–104
21. Kido A, Fujimoto K, Okada T, Togashi K (2013) Advanced MRI in malignant neoplasms of the uterus. JMRI 37:249–264
22. Sala EA, Rockall AG, Freeman SJ, Mitchell DG, Reinhold C (2013) The added role of MR imaging in treatment stratification of patient with gyne malignancies. Radiology 266:717–740
23. Freeman SJ, Aly AM, Kataoka MY, et al. (2012) The revised FIGO staging system for uterine malignancies: implications for MR imaging. Radiographics 32:1805–1827
24. Sala E, Wakely S, Senior E, Lomas D (2007) MRI of Malignant Neoplasms of the Uterine Corpus and Cervix. AJR 188:1577–1587
25. Sheu MH, Chang CY, Wang JH, Yen MS (2001) Preoperative staging of cervical carcinoma with MR imaging: a reappraisal of diagnostic accuracy and pitfalls. Eur Radiol 11:1828–1833
26. Togashi K, Nishimura K, Sagoh T, et al. (1989) Carcinoma of the cervix: staging with MR imaging. Radiology 171:245–251
27. Koyama T, Tamai K, Togashi K (2007) Staging of carcinoma of the uterine cervix and endometrium. Eur Radiol 17:2009–2019
28. Zand KR, Reinhold C, Abe H, et al. (2007) Magnetic resonance imaging of the cervix. Cancer Imaging 7:69–76
29. Qin Y, Peng Z, Lou J, et al. (2009) Discrepancies between clinical staging and pathological findings of operable cervical carcinoma with stage IB-IIB: a retrospective analysis of 818 patients. Aust N Z J Obstet Gynaecol 49:542–544
30. Lai CH, Yen TC, Ng KK (2010) Surgical and radiologic staging of cervical cancer. Curr Opin Obstet Gynecol 22:15–20
31. Bellomi M, Bonomo G, Landoni F, et al. (2005) Accuracy of computed tomography and magnetic resonance imaging in the detection of lymph node involvement in cervix carcinoma. Eur Radiol 15:2469–2474
32. Hori M, Kim T, Murakami T, et al. (2009) Uterine cervical carcinoma: preoperative staging with 3.0-T MR imaging–comparison with 1.5-T MR imaging. Radiology 251:96–104
33. Chung HH, Kang SB, Cho JY, et al. (2007) Can preoperative MRI accurately evaluate nodal and parametrial invasion in early stage cervical cancer? Jpn J Clin Oncol 37:370–375
34. Pandharipande PV, Choy G, del Carmen MG, et al. (2009) MRI and PET/CT for triaging stage IB clinically operable cervical cancer to appropriate therapy: decision analysis to assess patient outcomes. AJR 192:802–814
35. Lin G, Ho KC, Wang JJ, et al. (2008) Detection of lymph node metastasis in cervical and uterine cancers by diffusion-weighted magnetic resonance imaging at 3T. J Magn Reson Imaging 28:128–135
36. Chung HH, Kang KW, Cho JY, et al. (2010) Role of magnetic resonance imaging and positron emission tomography/computed tomography in preoperative lymph node detection of uterine cervical cancer. Am J Obstet Gynecol 203(156):e151–e155
37. Choi HJ, Roh JW, Seo SS, et al. (2006) Comparison of the accuracy of magnetic resonance imaging and positron emission tomography/computed tomography in the presurgical detection of lymph node metastases in patients with uterine cervical carcinoma: a prospective study. Cancer 106:914–922
38. Park W, Park YJ, Huh SJ, et al. (2005) The usefulness of MRI and PET imaging for the detection of parametrial involvement and lymph node metastasis in patients with cervical cancer. Jpn J Clin Oncol 35:260–264
39. Jeong YY, Kang HK, Chung TW, Seo JJ, Park JG (2003) Uterine cervical carcinoma after therapy: CT and MR imaging findings. Radiographics 23:969–981
40. Tanderup K, Georg D, Potter R, et al. (2010) Adaptive management of cervical cancer radiotherapy. Semin Radiat Oncol 20:121–129
41. Levy A, Caramella C, Chargar C, et al. (2011) Accuracy of Diffusion-Weighted Echo-Planar MR Imaging and ADC Mapping in the evaluation of residual Cervical Carcinoma after radiation therapy. Gynecol Oncol 123:110–115
42. Kim HS, Kim CK, Park BK, Huh SJ, Kim B (2013) Evaluation of therapeutic response to concurrent chemoradiotherapy in patients with cervical cancer using diffusion-weighted MR imaging. J Magn Reson Imaging 37:187–193
43. Kuang F, Yan Z, Wang J, Rao Z (2014) The value of diffusion-weighted MRI to evaluate the response to radiochemotherapy for cervical cancer. Magn Reson Imaging 32:342–349
44. Somoye G, Harry V, Semple S, et al. (2012) Early diffusion weighted magnetic resonance imaging can predict survival in women with locally advanced cancer of the cervix treated with combined chemo-radiation. Eur Radiol 22:2319–2327
45. Levy A, Medjhoul A, Caramella C, et al. (2011) Interest of diffusion-weighted echo-planar MR imaging and apparent diffusion coefficient mapping in gynecological malignancies: a review. J Magn Reson Imaging 33:1020–1027
46. Miccò M, Vargas HA, Burger IA, et al. (2014) Combined pretreatment MRI and 18F-FDG PET/CT parameters as prognostic biomarkers in patients with cervical cancer. Eur J Radiol 83:1169–1176
47. Wakefield JC, Downey K, Kyriazi S, deSouza NM (2013) New MR techniques in gynecologic cancer. Am J Roentgenol 200:249–260
48. Payne GS, Schmidt M, Morgan VA, et al. (2010) Evaluation of magnetic resonance diffusion and spectroscopy measurements as predictive biomarkers in stage 1 cervical cancer. Gynecol Oncol 116:246–252
49. Punwani S (2011) Contrast enhanced MR imaging of female pelvic cancers: established methods and emerging applications. Eur J Radiol 78:2–11
50. Charles-Edwards E, Messiou C, Morgan VA, et al. (2008) Diffusion weighted imaging in cervical cancer with an endovaginal technique: potential value for improving tumor detection in stage Ia and Ib1 disease. Radiology 249:541–550
51. Hricak H, Hamm B, Semelka RC, et al. (1991) Carcinoma of the uterus: use of gadopentetate dimeglumine in MR imaging. Radiology 181:95–106

52. Punwani S (2011) Diffusion weighted imaging of female pelvic cancers: concepts and clinical applications. Eur J Radiol 78:21–29
53. Signorelli M, Guerra L, Montanelli L, et al. (2011) Preoperative staging of cervical cancer: is 18-FDG-PET/CT really effective in patients with early stage disease? Gynecol Oncol 123:236–240
54. Grigsby PW, Siegel BA, Dehdashti F (2001) Lymph node staging by positron emission tomography in patients with carcinoma of the cervix. J Clin Oncol 19:3745–3749
55. Sironi S, Buda A, Picchio M, et al. (2006) Lymph node metastasis in patients with clinical early-stage cervical cancer: detection with integrated FDG PET/CT. Radiology 238:272–279
56. Reinhardt MJ, Ehritt-Braun C, Vogelgesang D, et al. (2001) Metastatic lymph nodes in patients with cervical cancer: detection with MR imaging and FDG PET. Radiology 218:776–782
57. Sakuragi N (2007) Up-to-date management of lymph node metastasis and the role of tailored lymphadenectomy in cervical cancer. Int J Clin Oncol 12:165–175
58. Ryu SY, Kim MH, Choi SC, Choi CW, Lee KH (2003) Detection of early recurrence with 18F-FDG PET in patients with cervical cancer. J Nucl Med 44:347–352
59. Choi J, Kim HJ, Jeong YH, et al. (2014) The role of (18) F-FDG PET/CT in assessing therapy response in cervix cancer after concurrent chemoradiation therapy. Nucl Med Mol Imaging 48:130–136
60. Kidd EA, Siegel BA, Dehdashti F, Grigsby PW (2007) The standardized uptake value for F-18 fluorodeoxyglucose is a sensitive predictive biomarker for cervical cancer treatment response and survival. Cancer 110:1738–1744
61. Weber WA (2005) Use of PET for monitoring cancer therapy and for predicting outcome. J Nucl Med 46:983–995
62. Soret M, Bacharach SL, Buvat I (2007) Partial-volume effect in PET tumor imaging. J Nucl Med 48:932–945
63. Kitajima K, Suenaga Y, Ueno Y, et al. (2014) Fusin of PET and MRI for staging of uterine cervical cancer: comparison with contrast-enhanced (18)F-FDG PET/CT and pelvic MRI. Clin Imaging 38:464–469
64. Kim SK, Choi HJ, Park SY, et al. (2009) Additional value of MR/PET fusion compared with PET/CT in the detection of lymph node metastases in cervical cancer patients. Eur J Cancer 45:2103–2109
65. Kidd EA, Siegel BA, Dehdashti F, et al. (2010) Lymph node staging by positron emission tomography in cervical cancer: relationship to prognosis. J Clin Oncol 28:2108–2113
66. Martínez A, Mery E, Filleron T, et al. (2013) Accuracy of intraoperative pathological examination of sentinel lymph node in cervical cancer. Gynecol Oncol 130:525–529
67. Agarwal S, Schmeler KM, Ramirez PT, et al. (2011) Outcomes of patients undergoing radical hysterectomy for cervical cancer of high-risk histological subtypes. Int J Gynecol Cancer 21:123–127
68. National Cancer Institute: NCI Clinical Announcement (1999) United States Department of Health and Human Services, Public Health Service, National Institutes of Health, Bethesda
69. Son H, Kositwattanarerk A, Hayes MP, et al. (2010) PET/CT evaluation of cervical cancer: spectrum of disease. Radiographics 30:1251–1268
70. Evans KD, Tulloss TA, Hall N (2007) 18FDG uptake in brown fat: potential for false positives. Radiol Technol 78:361–366
71. Subhas N, Patel PV, Pannu HK, et al. (2005) Imaging of pelvic malignancies with in-line FDG PET-CT: case examples and common pitfalls of FDG PET. Radiographics 25:1031–1043
72. Ulaner GA, Lyall A (2013) Identifying and Distinguishing Treatment Effects and Complications from Malignancy at FDG PET/CT. Radiographics 33:1817–1834
73. Treglia G, Taralli S, Salsano M, et al. (2014) Prevalence and malignancy risk of focal colorectal incidental uptake detected by (18)F-FDG-PET or PET/CT: a meta-analysis. Radiol Oncol 48:99–104
74. Israel O, Yefremov N, Bar-Shalom R, et al. (2005) PET/CT detection of unexpected gastrointestinal foci of 18F-FDG uptake: incidence, localization patterns, and clinical significance. J Nucl Med 46:758–762
75. Sudderuddin S, Helbren E, Telesca M, Williamson R, Rockall A (2014) MRI appearances of benign uterine disease. Clin Radiol 69:1095–1104
76. Allen BC, Hosseinzadeh K, Qasem SA, Varner A, Leyendecker JR (2014) Practical approach to MRI of female pelvic masses. Am J Roentgenol 202:1366–1375
77. Fayad LM, Cohade C, Wahl RL, Fishman EK (2003) Sacral Fractures: A Potential Pitfall of FDG Positron Emission Tomography. American Journal of Roentgenology 181:1239–1243
78. Rolton DJ, Blagg SE, Hughes RJ (2011) Osteoradionecrosis of the lumbar spine 25 years after radiotherapy. J Bone Joint Surg 93:1279–1281
79. Salavati A, Shah V, Wang ZJ, et al. (2011) F-18 FDG PET/CT findings in postradiation pelvic insufficiency fracture. Clin Imaging 35:139–142